NUST COLLEGE OF

ELECTRICAL AND MECHANICAL ENGINEERING

Study on the impact strength of 3D printed thermoplastic polymers subjected to post-printing heat-treatments

A PROJECT REPORT

DE-40(DME)

Submitted by

Syed Muhammad Asad Abbas Rizvi

Nadeem Ahmed

Muhammad Ahmad

Muhammad Zauraiz Abdullah

BACHELORS

IN

MECHANICAL ENGINEERING

Year

2022

PROJECT SUPERVISOR

Dr. Bilal Anjum

CO-SUPERVISOR

Lec. Usman Zia

NUST COLLEGE OF ELECTRICAL AND MECHANICAL ENGINEERING

PESHAWAR ROAD, RAWALPINDI

DECLARATION

We hereby declare that no portion of the work referred to in this Project Thesis has been submitted in support of an application for another degree or qualification of this of any other university or other institute of learning. If any act of plagiarism found, we are fully responsible for every disciplinary action taken against us depending upon the seriousness of the proven offence, even the cancellation of our degree.

COPYRIGHT STATEMENT

ACKNOWLEDGEMENTS

We are thankful to Allah Almighty, the most merciful and Al Fattah, for the blessings, courage, and the intellect He has bestowed us with, because of which it became possible for us to accomplish such remarkable goal.

We are thankful to our parents and the family for their constant support and encouragement through each thick and thin. We are much obliged to our supervisor Dr. Bilal Anjum and Co-supervisor Sir Usman Zia for their continuous guidance and the valuable time they spent on providing us the support and the encouragement through each stage. without their efforts we would have never been able to achieve that much. Moreover, we are grateful to all our fellows, friends who supported us intellectually and emotionally. Tones of thanks for all those who contributed in it, without all that support and appreciation things would have been different. We are hopeful that this project will add value to the peoples' life and would be developed further to adopt this technology on the massive level

Table of Contents

List Of Tables:

List of Figures

ABSTRACT

Thermoplastic polymers can be softened and melted by heating which helps in molding them in different shapes. They are highly recyclable. Parts made from these thermoplastic polymers fabricated through 3D printing have reduced mechanical properties compared to those fabricated through injection molding. In this study, 3D printed samples manufactured using PLA and ABS filaments were subjected to impact testing. The samples were prepared by varying raster angle (0˚-90˚) and build orientation (horizontal and vertical). Moreover, effect of post-printing heat treatment on the impact strength of samples was also studied. Samples printed in vertical orientation had the lowest impact strength and a flat fracture, owing to weak inter-layer bonding. Whereas impact strength was seen to increase with the increase in raster angle due to better adhesion between neighboring fibers. Poor interlayer tensile strength and void formation are some of the common defects associated with 3D printing. These defects are the main reason for the low impact strength of 3D printed parts. Heat-treatment of the samples 35-45 degrees above the glass transition temperature resulted in significant improvement in the impact strength of all the samples. The improvement is owed to improved adhesion between the neighboring layers and raster. The fractured surfaces are observed, and the defects are noted both with and without heat treatment. This work basically analyzes a post-processing heat treatment aimed at enhancing mechanical properties of 3D printed parts, while minimizing the associated defects. More specifically, purpose of this project is to study the impact strength of 3D printed thermoplastic polymers subjected to post printing heat treatment process and understanding the effect of heat treatment on structural changes.

CHAPTER 1: INTRODUCTION

Since the origination of three-dimensional (3D) printing around 40 years ago, there has been the expansion of a few additive manufacturing (AM) advances that empower its utilization in ordinary applications like aviation, medication, military, oil and gas and foundation. In order to improve its applicability and growth, 3D printed materials are subjected to the same or even higher levels of scrutiny on its mechanical behavior as the conventionally manufactured counterpart. One of the most significant mechanical properties is strength or the capacity of a material to go through large amount of strain prior to fracture when loaded. The durability of a material can be associated to its impact energy or the increment in internal energy due to impact. Impact strength is the ability of a material to withstand a suddenly applied load. Ductile materials have more impact energy and thus there impact strength is high. In this study the impact properties of thermoplastic polymers are investigated by using Charpy impact test. Thermoplastic polymers can be softened and melted by heating which helps in molding them in different shapes. They are highly recyclable. Parts made from these thermoplastic polymers fabricated through 3D printing have reduced mechanical properties compared to those fabricated through injection molding. Poor interlayer tensile strength and void formation are some of the common defects associated with 3D printing. It is reported that environmental conditions and heating treatment have profound influence on the mechanical properties of theses polymers. This work would analyze a post-processing heat treatment aimed at enhancing mechanical properties of 3D printed parts, while minimizing the associated defects.

3D printing is a method used to make the 3-dimensional advanced models, ordinarily by setting down numerous progressive thin layers of material. Many conventional methods have been used to design a product with given specifications for real-time applications. The drawbacks with those methods included not cost-effective and utilizing more time and energy. 3D printing is a technique which can replace the previous conventional methods. Polylactic acid (PLA), Acrylonitrile Butadiene Styrene (ABS) and Nylon are some of the materials used to print the objects. Printing techniques were broadly classified into seven types: Stereolithography (SLA), Selective Laser Sintering (SLS), Selective Laser Melting (SLM), Fused Deposition Modelling (FDM), Digital Light Processing (DLP), Electron Beam Melting (EBM) and Laminated Object Manufacturing (LOM). In the current research, we used FDM technique to print the samples.

Fused Deposition Modelling, otherwise called fused filament fabrication is used to manufacture an item with the help of a filament coil associated with a heated extruder. The extruder will move in the x and y headings on the structure stage to form the object. The fiber material which was taken care of into the extruder will be warmed up in the nozzle and hardens rapidly after deposition. After consummation of each layer, the structure stage drops down so the nozzle can print the following layer on top of the earlier. The interaction proceeds by adding layers until the sample is finished. A portion of the advantages of FDM are it very well may be utilized to print complex items utilizing various materials, it is not difficult to replace filament materials in a brief time frame, and it is conceivable to print with less expensive materials.

ABS is one such material which is broadly utilized in added substance fabricating. It is a dark thermoplastic polymer with high strength and solidness and simplicity of handling. Products with ABS are normally prepared by extrusion or injection molding. It has promising effect obstruction and durability although the properties might be fluctuated dependent on the last handling conditions like temperature and strategy for handling. Anyway, in additive manufacturing (AM) processes, the properties of a completed item are administered by different boundaries like raster direction, air gap, binder saturation, layer thickness and so on, rather than the material properties. ABS is a common thermoplastic polymer. Its glass transition temperature is approximately 105 °C (221 °F). ABS is amorphous and therefore has no true melting point. ABS is a terpolymer made by polymerizing styrene and acrylonitrile in the presence of polybutadiene. The proportions can vary from 15 to 35% acrylonitrile, 5 to 30% butadiene and 40 to 60% styrene. The result is a long chain of polybutadiene crisscrossed with shorter chains of poly(styrene-co-acrylonitrile). The nitrile groups from neighboring chains, being polar, attract each other and bind the chains together, making ABS stronger than pure polystyrene. The styrene gives the plastic a shiny, impervious surface. The polybutadiene, a rubbery substance, provides toughness even at low temperatures. For the majority of applications, ABS can be used between −20 and 80 °C (−4 and 176 °F) as its mechanical properties vary with temperature The properties are created by rubber toughening, where fine particles of elastomer are distributed throughout the rigid matrix.

PLA is ring-opening polymerization of lactide with various metal catalysts either in a solution or as a suspension. The metal-catalyzed reaction tends to lead to racemization of the PLA, which reduces stereoregularity when compared to the biomass starting material. It is also possible to

produce PLA through the direct condensation of lactic acid monomers. Heat resistant PLA can withstand temperatures of 110 °C, and the melting temperature can be increased by 40–50 °C and the heat deflection temperature can be increased from around 60 °C to as much as 190 °C by physically blending the polymer with PDLA. It is widely used as a 3D printing feedstock for desktop fused filament fabrication 3D printers. PLA is popular for 3D printing as it can easily be sanded, painted, or post processed. A user-friendly material, this plastic works with low extrusion temperatures and there is no need for a heated bed, printer chamber or reinforced nozzle. (PLA) is a biodegradable and bioactive thermoplastic aliphatic polyester derived from renewable biomass, typically from fermented plant starch such as from corn, cassava, sugarcane, or sugar beet pulp. In 2010, PLA had the second highest consumption volume of any bioplastic of the world. The name "polylactic acid" does not comply with IUPAC standard nomenclature, and is potentially ambiguous or confusing, because PLA is not a polyacid (polyelectrolyte), but rather a polyester.

Table 1. Properties of PLA vs. ABS

PROPERTIES	**ABS**	**PLA**
Tensile Strength	27 MPa	37 MPa
Elongation	3.5-5.0%	6%
Flexural Modulus	2.1-7.6GPa	4GPa
Density	1.0-1.4g/cm^3	1.3g/cm^3
Melting Point	200°C	173°C
Biodegradable No	Yes	Under the correct conditions
Glass Transition Temperature	105°C	60°C

CHAPTER 2: LITERATURE REVIEW

PLA and ABS are both thermoplastics. PLA is stronger and stiffer than ABS, but poor heat-resistance properties mean PLA is mostly a hobbyist material. ABS is weaker and less rigid, but also tougher and lighter, making it a better plastic for prototyping applications. PLA is a user-friendly thermoplastic with a higher strength and stiffness than ABS. With a low melting temperature and minimal warping, PLA is one of the easiest materials to 3D print successfully. Unfortunately, its low melting point also causes it to lose virtually all stiffness and strength at temperatures above 50 degrees Celsius. In addition, PLA is brittle, leading to parts with poor durability and impact resistance. Although PLA is the strongest of the two plastics, its poor chemical and heat resistance force it into almost exclusively hobbyist applications.

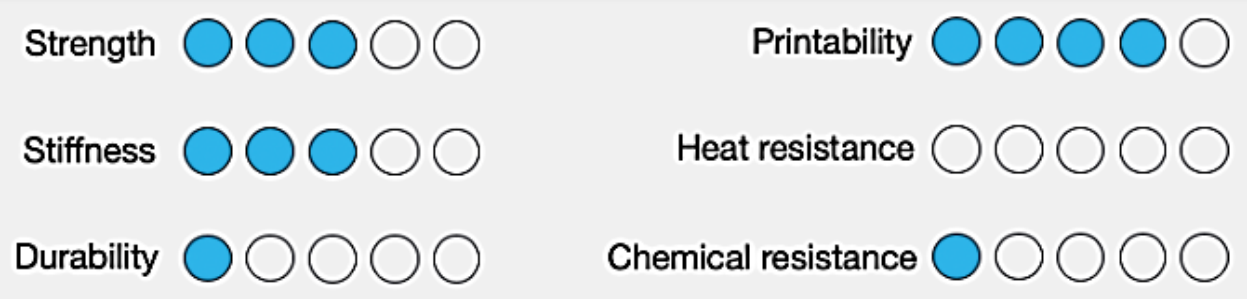

Figure 1: Mechanical properties of PLA [1].

ABS, while weaker and less rigid than PLA, is a tougher, lighter filament more suitable for some applications beyond purely hobbyist. ABS is a bit more durable, is about 25% lighter, and has four times higher impact resistance. ABS do require more effort to print than PLA because it's more heat resistant and prone to warping. This calls for a heated bed and an extruder that is 40-50 degrees Celsius hotter. ABS, while by no means a heat resistant plastic, has superior heat deflection temperature compared to PLA. The improved durability over PLA lends ABS to some more practical applications, such as prototyping and low-stress end-use parts.

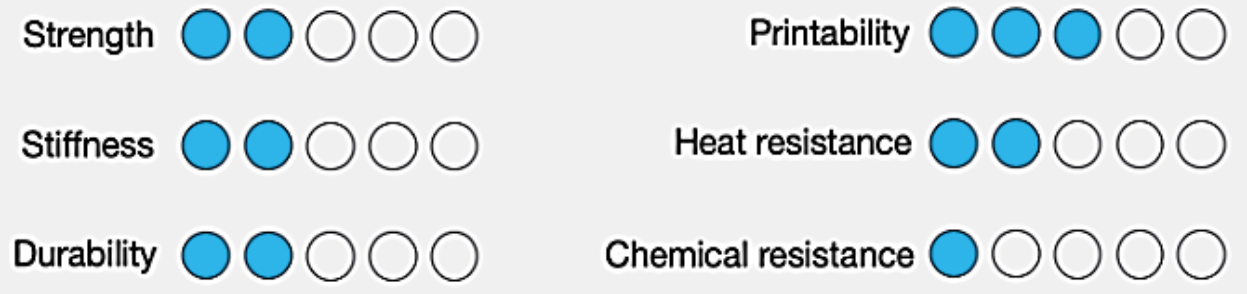

Figure 2: Mechanical Properties of ABS [2].

2.1: Injection Molding and Fused Deposition Modeling:

An additive manufacturing (AM) plays an essential role in economic competitiveness. 3D printing with reference to AM is enabling technology for a wide range of new polymer products . This method is currently reforming the commercial manufacturing sector for the polymer industry and aims to replace the injection molding where the problems of melt line and weld line when the materials meet up within the mold could be overcome. Furthermore, injection molding has others limitations such as it has a high initial tooling cost, part design restrictions, and complex fabrication methods.

Fused deposition modeling (FDM) is the most commonly used 3D printing method for thermoplastics materials, mainly due to its ease of handling, rapid processing, simplicity, and cost-efficiency. FDM is a simple additive manufacturing technology in which a thermoplastic filament is extruded through a circular nozzle to build 3D objects layer by layer . The FDM method has the ability to manufacture complex structures with satisfactory sizes, and geometric accuracy without much waste being generated. The materials have to be in a filament form, and the molten viscosity should be high enough to provide structural support but low enough to enable the extrusion. Most polymers such as ABS ,PLA, polyamide, polycarbonate (PC), high density polyethylene (HDPE), and polyurethane (PU) are fabricated using FDM. However, polymer products fabricated using this method lack strength due to the presence of voids caused by incomplete diffusion at the interfaces during fabrication. [3].

Fused deposition modelling (FDM) is the most commonly used 3D printing method for thermoplastics materials, mainly due to its ease of handling, rapid processing, simplicity, and cost-efficiency. FDM is a simple additive manufacturing technology in which

a thermoplastic filament is extruded through a circular nozzle to build 3D objects layer by layer . The FDM method has the ability to manufacture complex structures with satisfactory sizes, and geometric accuracy without much waste being generated. The materials have to be in a filament form, and the molten viscosity should be high enough to provide structural support but low enough to enable the extrusion. Most polymers such as ABS ,PLA, polyamide, polycarbonate (PC), high density polyethylene (HDPE), and polyurethane (PU) are fabricated using FDM. However, polymer products fabricated using this method lack strength due to the presence of voids caused by incomplete diffusion at the interfaces during fabrication.

A number of studies have been reported regarding the modification of the processing parameters such as air gaps, raster width, and raster angle ; layer thickness, infill orientation, and shell wall thickness; and layer height and orientation, infill density, and plate and extruder temperature to improve the properties of the final product. It was found that the mechanical properties of the polymers could be improved with a raster angle of 0/90° and a layer height of 0.1–0.2 mm. Equable et al. employed the Taguchi method to optimize the layer thickness and raster orientation of some FDM products. Work by Wang et al. suggested that the values of the shells and air gaps at 1 and 0 mm, respectively are able to improve the mechanical properties of the final product. Moreover, Aw et al. observed that a combination of different line patterns and 100% infill density reduced the gap between the printed lines and increased adhesion between the top and bottom layers. This improved the ability of the products to deform and absorb stress before it breaks. Although numerous investigations have been carried out to optimize FDM processing parameters to produce products with improved performance, a problem, however, remains the expected depreciation in physical and mechanical properties in contrast to the injected products.

Figure 3 shows the tensile properties of different types of thermoplastics fabricated using FDM and injection molding. The tensile strength of FDM printed PLA and ABS are found to be 48% and 34%, lower compared to those fabricated using injection molding. Generally, samples from the injection molding are injected at high pressure which promotes an excellent entanglement of polymer chains, resulting in strong and stiff materials. In addition, the increase of temperature inside the barrel creates a symmetrical flow during the filling of the mold which increases the modulus of the samples. On the other hand, in the layer by layer FDM process, the top and bottom filaments typically do not attach perfectly and bond to each other, leading to the formation of air

pockets and porous structures containing large gaps between the strands. These results are correlated with the reduction of density and increment of water absorption as discussed previously. Moreover, if the printing process is paused to insert a new filament, the gaps between the printed filaments become larger and cause reduced bonding between each layer. It is expected that the *z*-printing direction helps to increase the strength of the samples, but the tensile properties were reduced which could be caused by a non-planar breakage of the samples at the intersection of the layers and randomly orientation of the filament during printing as stated by Wang et al.

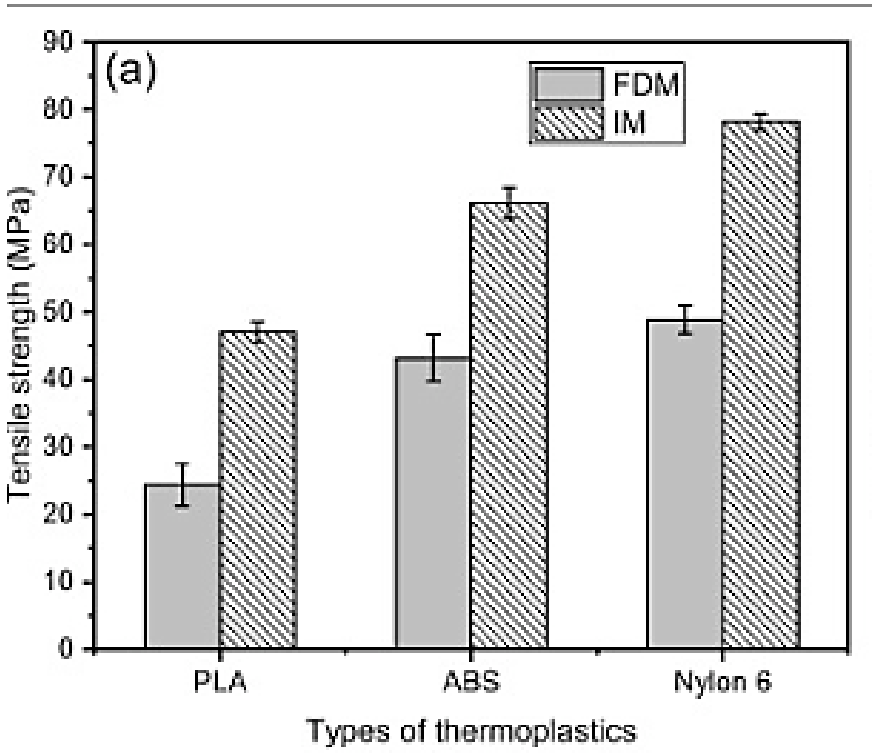

Figure. 3 Mechanical properties of thermoplastics from FDM and injection molding: tensile strength. [4].

In Figure 4, it is shown that Young's modulus of ABS and nylon 6 fabricated using FDM are comparable with the injection molded samples with percentage differences of 18.9%, and 14.5%, respectively. This could be due to the consistency of high infill density, leading to high adhesion of bonding between the printed layers which makes the structure denser, thus increasing the stiffness of the samples. It has consistent results due to its higher melting point which helps the filament hold its shape better than others. Young's modulus of PLA fabricated using FDM is 47.2% lower than the injection molded sample. The use of the extruder temperatures for PLA at 210 °C

decreases the viscosity of the molten polymer, such that the extruded materials lose its sectional circular shape, leading delamination between layers.

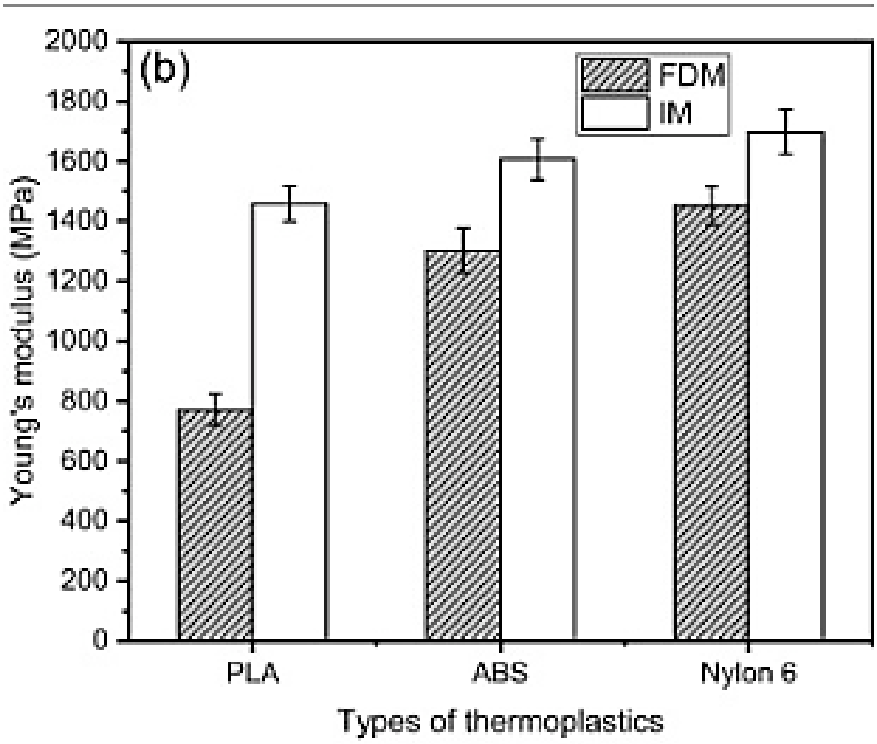

Figure 4 : Mechanical properties of thermoplastics from FDM and injection molding: Young's Modulus [5].

Elongation at break of the FDM printed and injection molded samples are presented in Figure 5. The percentage differences of elongation at break of PLA, ABS, from both methods are 32.9%, 50.8%, respectively. In FDM, the strain of samples mainly relies on the raster angle in which the direction of the raster is inconsistent at x-axis of the plate. Moreover, the formation of microcracks on the surface of the samples together with the gaps between the filaments contributes to poor adhesion between the layers. This, in turn, reduces the strain required to break the materials. The use of constant temperature during the injection process induces the entanglement of polymer chains. As a result, the injected samples are able to elongate further before reaching the breaking point.

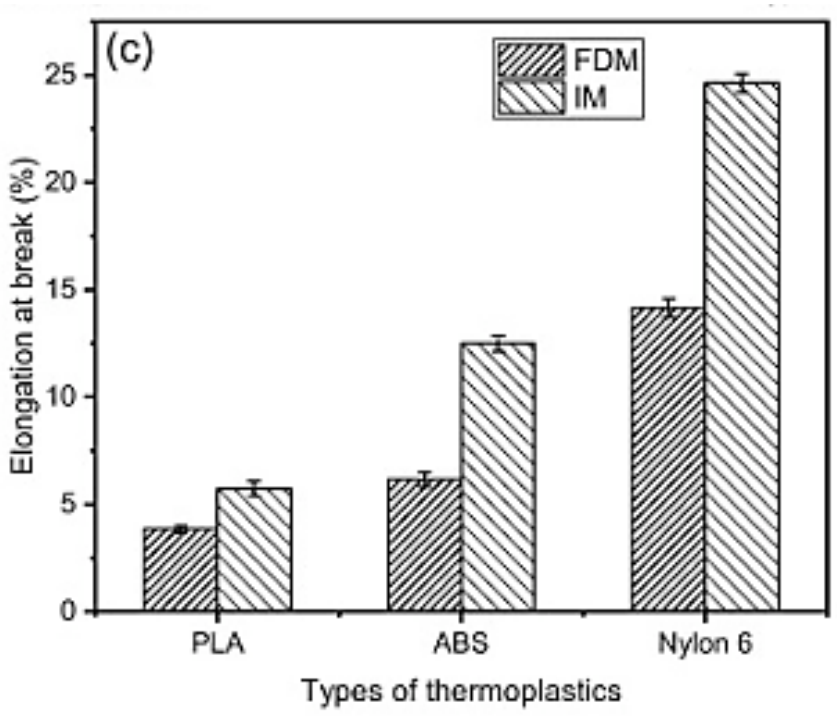

Figure 5 : Mechanical properties of thermoplastics from FDM and injection molding: Elongation at break [6].

The impact strength of all samples fabricated by FDM, and injection molding is displayed in Figure 6. The impact strength of FDM printed samples is low compared to the injection molded samples. However, the values obtained for PLA and ABS were higher compared to those reported elsewhere. The reduction of the impact strength in FDM's printed samples could again be explained due to inconsistent plate temperature which could potentially create small diffusion with large voids. Wang et al. suggest that the diffusion is larger with higher plate temperature leading to the small size of the voids on the surface of the samples. Recently, Bentwood et al. found that the optimum plate temperature for PLA is 105 °C, and the prolonged cooling time helps to reduce the voids and enhance adhesion between the layers.

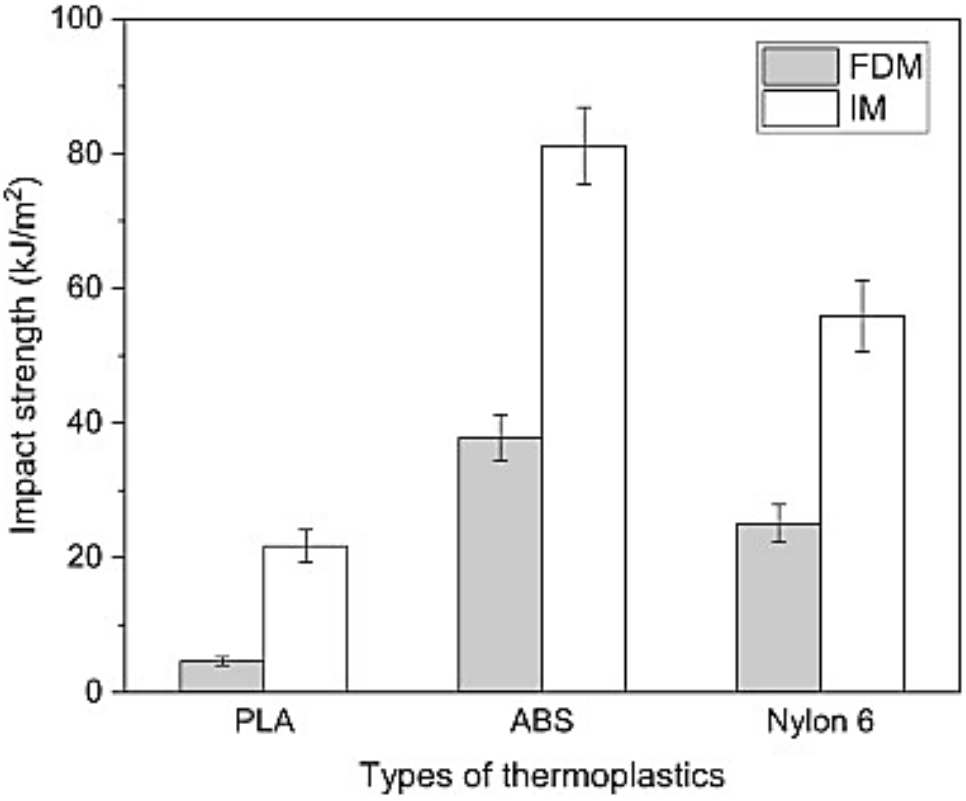

Figure 6: Impact strength of thermoplastics from FDM and injection molding [7].

Another factor that results in lower impact strength for FDM samples is higher moisture absorption on the filament surface. Although the pallets for FDM and injection molding dry at similar time and temperature, the slow feed rate of the filament during FDM exposes it to air moisture for a long period of time. Evidence of vaporization of the physically absorbed water at the surface of the samples was calculated and the TGA analysis indicates a slight weight loss between 100 °C and 280 °C, as illustrated in the table 2. On the other hand, the high impact strength of the injection molded samples can be attributed to the optimum processing by controlling the mold temperature and preventing moisture absorption inside the barrel [8].

Table 2: Weight loss of FDM printed and injection molded samples at 200 °C

Materials	FDM	Injection Molding
PLA	0.62	0.78
ABS	0.76	0.81

2.2: Optimization of Print Process:

Benwood et al. (2018) investigated the effect on mechanical properties of PLA by changing the thermal conditions of the printing process. In his study, samples were printed with different bed and melting temperatures and later impact tested for strength. Surprisingly, they reported that samples printed with high bed and melting temperatures showed a low porosity but improved density characteristics and crystallinity changes. The impact strength of the samples printed with high melt and bed temperatures showed high impact 39 strengths. The results are shown in figure 7 below. So, this confirms print parameters also play an important role in optimization of mechanical properties of PLA.

Trial	Nozzle Temperature	Platform Temperature	Severity of voids
1	185°C	40°C	185
2	190°C	45°C	190
3	195°C	45°C	195
4	200°C	45°C	200
5	205°C	45°C	205
6	210°C	50°C	210
7	215°C	50°C	215

Figure 7: Shows the severity of voids at different nozzle and platform temperatures [9].

A study was done by Lu Wang et al. (2017) to improve the impact strength of PLA in Fused deposition modelling (FDM). In that study, two printing parameters, layer height (0.2mm and 0.4mm) and platform temperature (30 and 160 ºC) were investigated for their effect on the impact strength of printed PLA. According to their fused layer model, a proper selection of printing parameters can produce a high impact Trial Nozzle Temperature (185ºC-215ºC) Platform temperature (40ºC-50ºC) and Severity of Voids. Scanning electron Microscopy (SEM) showed a layer height of 0.2mm and platform temperature of 160ºC produced fewer voids and large impact resistance. Additionally, Size exclusion Chromatography (SEC) was applied to study the molecular weight change of PLA observed from different processes. It was shown that degradation as evidenced by molecular weight changes is higher in injected molded PLA when compared with

printed PLA. Tahseen. F.D and Farhad M.H (Abbas and Othman 2018) investigated the effect of layer thickness on the impact properties of 3D printed PLA. In that research, samples were printed with fused deposition technique and different layer thicknesses; 0.1mm, 0.15mm, 0.2mm, 0.25mm, and 0.3mm. These samples were tested for impact properties by the standard Izod method. They reported that the smaller the layer thickness, the higher the impact strength with the lowest impact strength being recorded for the sample with the highest layer thickness i.e., 0.3mm. The time taken to build the sample with 0.1mm layer thickness was higher when compared to the sample printed with 0.3mm thickness.

2.3: Effect of Printing Parameters on Mechanical Properties:

The values for the printing process parameters are carefully selected based on the part's application. These are the most common FDM printing process parameters, along with their variables and ranges:

Raster angle, sometimes called raster orientation, is the direction of the deposited layers with respect to the build platform. It usually ranges from 0◦ to 90◦. Zhang et al. studied the effects of raster angle on the mechanical properties of PLA parts produced using FDM. They concluded that raster angle significantly affects the different mechanical properties of PLA, as illustrated in Figure 8 a–c. Algarni investigated the effects of raster angle on PLA samples and concluded that the UTS was affected significantly by the raster angle such that it dropped by 36% when the raster angle changed from 0° to 90°. Similarly, Young's modulus and elongation at break decreased by 9% and 14% respectively.

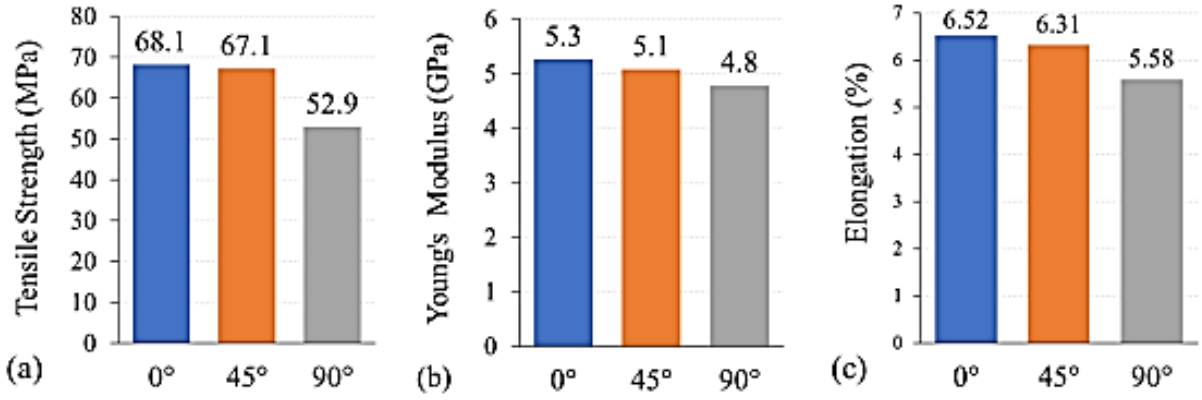

Figure 8. Influence of raster angle on PLA (a) tensile strength, (b) Young's modulus, and (c) % elongation [11].

Fatimatuzahraa et al. studied the effects of different raster angles on the mechanical properties of FDM parts made of ABS material. They defined the raster angles as follows: axial (0◦), crisscross (45◦/−45◦), cross (0/90◦), and transverse (90◦). The cross and crisscross samples exhibited negligible differences in tensile strengths of 18.5 MPa and 18.3 MPa, respectively. The findings of the study ae summarized in Figure 9 a, b. [10].

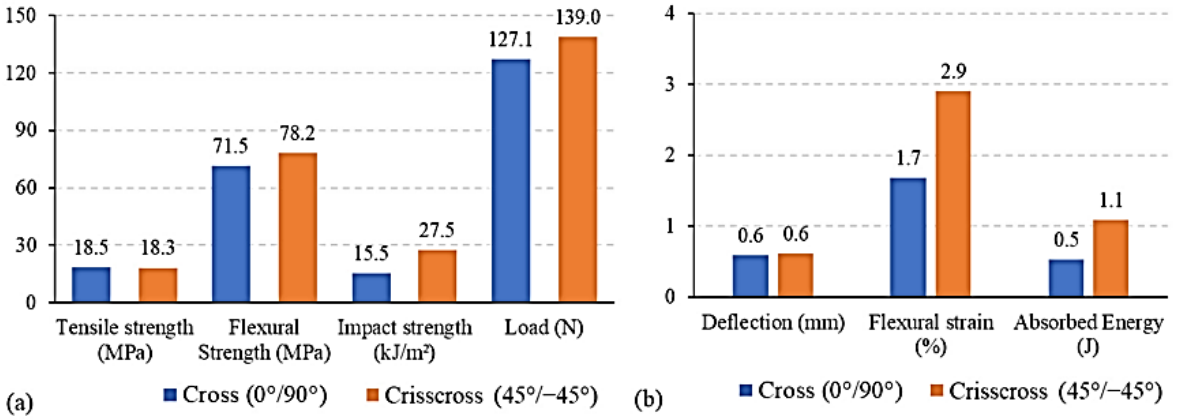

Figure 9. Effects of raster angle on different mechanical properties (a) and (b) of ABS [12].

Panes et al. studied the effects of different manufacturing parameters on the mechanical behaviors of PLA parts fabricated via FDM methods. The study concluded that increasing the infill percentage from 20% to 50% improved the UTS by 27%, yield stress by 21%, Young's modulus by 34% and elongation at break by 30%. A study by Rismalia et al. shows that increasing the PLA infill percentage from 25% to 75% could enhance the UTS, yield strength, and the modulus of elasticity by 40%, 34%, and 15%, respectively. Baich et al. studied the effects of infill percentage on mechanical strength and print costs for 3D printed ABS parts produced using infill percentages of 50%, 75%, and 100%. They found that samples produced with 100% infill outperform samples produced with 50% infills for all mechanical properties. Furthermore, a study by Panes et al. concluded that increasing the infill percentage from 20% to 50% for ABS improves its UTS by 26%, yield stress by 24%, Young's modulus by 45% and elongation at break by 1% [13 – 15].

Diverse printing speeds impact the material's spread and shaping aspect. In small parts, high printing speed leads to material deformations because of new layers being put on top of layers that poor person yet completely set. Therefore, the heaviness of the new layer distorts the previous

layer. Printing speed influences statement width more than it does on the testimony stature. Moreover, scientists have concluded that higher printing speed somewhat decreases the tensile strength. A study in this regard shows that different printing speeds (70, 80, 90, 100, and 110 mm/s) do not change young's modulus by more than 20%. Additionally, higher printing speeds affect how the filament melts and causes poor layer-to-layer adhesion, which results in lower strength. A study on ABS examined the effects of three different printing speeds (30, 35, and 40 mm/s) on tensile strength. The study arrived at similar results: the tensile strength dropped from 15.5 MPa to 13.7 MPa [16, 17].

2.4: Effect of Heat Treatment on Mechanical Properties:

Alain Copinet et al. (2004) studied the effect of temperature, ultra-violet light (315nm) and relative humidity (RH) on the degradation of PLA. Samples were prepared by placing PLA in Erlenmeyer flasks containing a universal stopper and a chloroform solution and then dried on glass to produce PLA films. Fourier transform infrared spectrograph (FTIR) technique was used to identify the degradation process in samples. The paper concluded that UV light has a larger impact on the degradation of PLA films compared to temperature or humidity. An increase of temperature and RH accelerated the degradation process and decreased polymer properties such as molecular weight (Mw) and glass transition temperature. The reasons given for this decrease included absorption of water which resulted in the hydrolysis process occurring within the samples. Hydrolysis is a process that when a substance reacts with water it breaks down large macromolecules into smaller components and this process increases with the increase of temperature. By using FTIR technique, it was observed that an increase of temperature and degradation the sample increased its crystallinity behavior in polymer chains.

Kai-Lai G. Ho et al. (1999) studied the degradation of three high molecular weight PLA films. They investigated films at different environmental parameters such as temperature (28, 40 and 55ºC) and relative humidity (10%, 50%, and 100%). Chronopol (Ch-I) and Cargill Dow polymers such as GII and Ca-I were chosen and tested. The results show a decrease in tensile properties of PLA films when their average Mw was in the range of 7 50k-75k g mol-1. From all testing results, Ca-I reported the lowest degradation rate when compared to Ch-II and GII. GII recorded the fastest

degradation rate of 27,361 Mw/week. They also observed that the degradation rate of plastic increased with the increase of temperature and relative humidity (RH).

Niaounakis et al. (2010) sought to investigate the behavior of environmental parameters such as temperature and relative humidity in the aging of PLA. The tested temperature conditions were 20, 40 and 50ºC and relative humidity of 80%. The samples were exposed to two heating runs of each of the environmental conditions at different aging periods (30, 60, 80, 100, and 130 days). The PLA samples were tested with various techniques, including size exclusion chromatography, dynamic mechanical analysis, and differential scanning calorimetry. They observed that reduction of properties happened to samples exposed at 20ºC for 30 days, but no further loss was seen at 40ºC. An intense decrease in properties occurred to the samples at 50ºC for 100 days. They concluded that the rate of degradation was slow for samples exposed under or equal to 40ºC, but the rate increases when the temperature was above 50ºC [18].

CHAPTER 3: DEFECTS IN 3D PRINTING

3.1: Injection Molding and Fused Deposition Modeling:

Figure 10 shows the SEM microstructures of the fabricated samples using FDM and injection molding. It can be clearly seen that all the samples fabricated using FDM have high void contents with gaps between the layers. This can be attributed to the uneven distribution of polymer melts during the extrusion of the filament and poor adhesion between the layers. In contrary, the injection molded samples have a rough fracture surface with a tearing line due to a constant mold pressure, resulting in a high degree of mold filling. Moreover, an injection molding process is conducted at a constant range of processing temperature which forms compactness of the materials inside the mold. The high packing pressure leads to a high concentration of flow in the mold, and subsequently, the molten polymers are able to completely fill the mold and form tight bonds between each polymer chain.

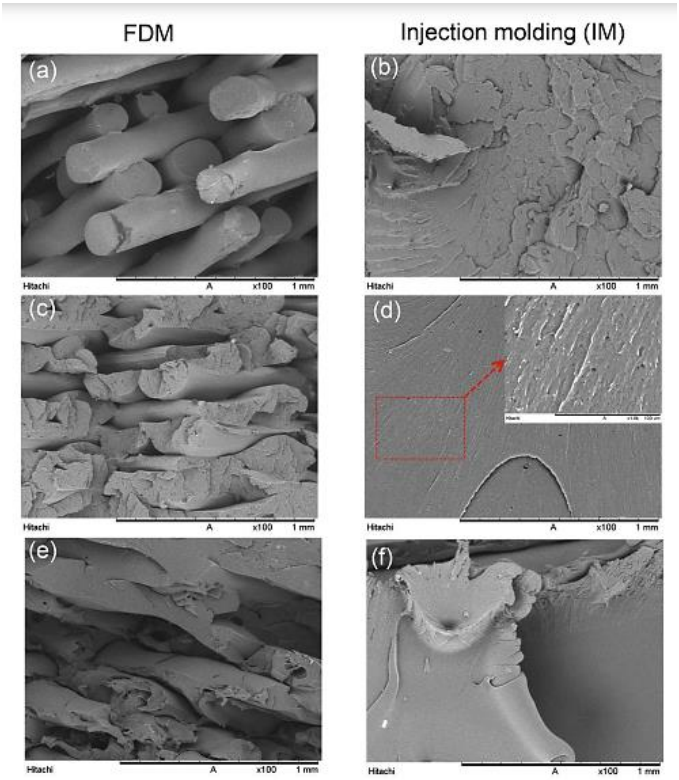

Figure 10. SEM of fractured surface of (a–b) PLA, (c–d) ABS, and (e–f) nylon 6 using FDM and injection molding, respectively at 100× magnification, and enlarge of ABS (d) at 1 KX magnification [19].

The degree of crystallinity for different types of thermoplastics fabricated using FDM and injection molding is shown in Figure 11. It can be seen that the FDM printed and injected ABS have the same broad peak at 19.8° which indicate amorphous behavior. The persistent amorphous peak of ABS filament helps maintain the viscosity in the nozzle and prevent freeze off or drooling during the FDM process. The fabricated methods used here, however, affect the peak height and width of the semi-crystalline PLA and nylon 6. For injection molded PLA, the amorphous behavior was represented by a broadened halo at 16.5° without any significant peak, while the FDM printed samples appear to have a sharp peak of crystal structure at 16.7°. This is in agreement with the report made by another researcher. A sharp crystal peak for FDM printed PLA could be related to the reordering of chains in the amorphous region, thus increasing the crystallinity of the sample. Zhang et al. stated that the PLA crystals can be potentially induced when the crystallization temperature is above 120 °C during the FDM process. It can be further explained that this could be due to the variation of nozzle temperature during printing where the temperature was high above the cold crystallization temperature (T_{cc}) when the nozzle moves close to the sample and drops down to below T_{cc} when the nozzle moves away. The quick heating and cooling cycles create more nucleation and smaller crystals instead of enlarging a single crystal.

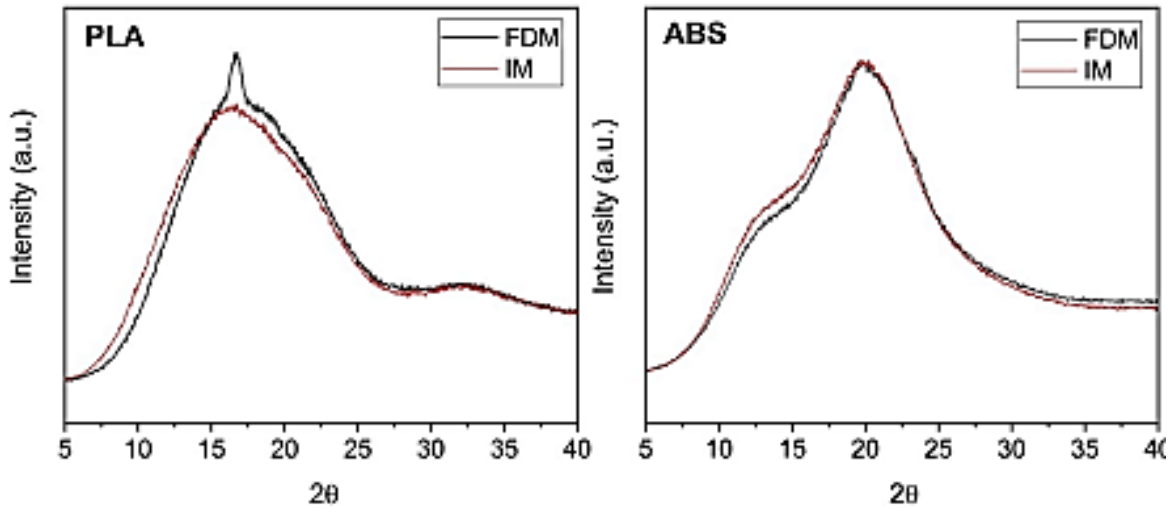

Figure 11. XRD patterns of PLA, ABS, and nylon 6 from FDM and injection molding[20].

3.2: Defects due to Mechanical Properties in FDM observed in SEM:

As per many research works, it has been clearly identified that there are a few drawbacks in FDM printed polymers that cannot be rectified only by engaging optimal printing parameters. These drawbacks directly affect the strength and appearance of the printed part. Generally, these defects can be summarized as shape distortion that occurs due to residual stresses caused by non-uniform temperature gradients, micro voids in the filaments, uneven fiber distribution within the fiber-reinforced thermoplastic filament, poor bonding between fibers and surface roughness occurring due to the staircase effect. Some of the void formation in FDM is inevitable due to the nature of this printing process. The voids between the layers are much bigger and differ with the airgap and layer thickness of the print, while the voids present inside the filament are much smaller and difficult to control by changing printing parameters. According to many experiments, it has been identified that the gaps between the layers, which contribute to the failure of the printed part by delamination, can be reduced by minimizing the layer thickness. It is evident from the figure below that the voids between layers could be minimized by reducing the layer thickness. Figure 12 a,b shows the effect of layer thickness on the void formation, and it is evident that the voids between layers could be minimized by reducing the layer thickness. The layer thickness in FDM typically lies within the range of 0.05 mm–0.4 mm. Even though a finer layer thickness minimizes the void content in the FDM printed part, it negatively affects the production time. When the layer thickness is small, the number of layers required to complete the part increases; hence, the production time will also increase. Several experiments have observed many void formations within the extruded filament, which were smaller than 16.4 μm, and they greatly affected the porosity percentage in the printed part. When the stress is concentrated on those weak void areas, it causes premature failure in the specimen [21,22].

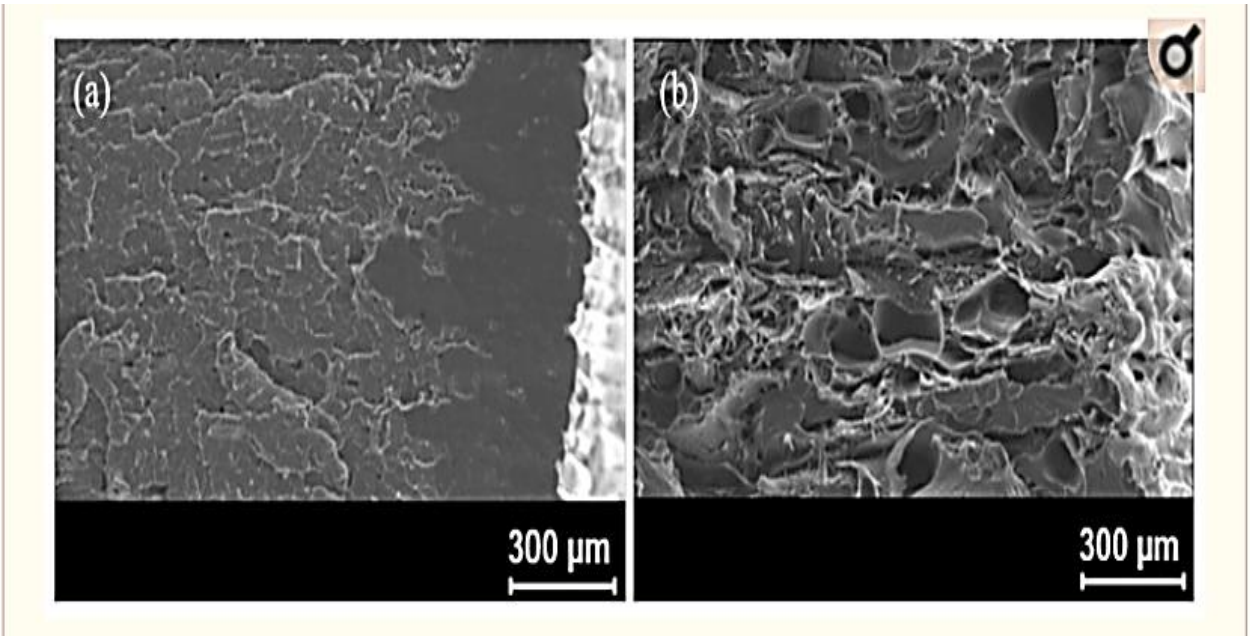

Figure 12: (**a**) ABS print cross-section with a layer thickness of 0.06 mm. (**b**) ABS cross-section with a layer thickness of 0.17 mm. The increased layer thickness caused many voids [23].

He et al. identified a large distribution of voids near the crack initiation point and recorded poor resistance to crack growth within those void areas. These micro voids are one of the main reasons for the poor strength exhibited by parts printed with the FDM process. Aside from the mechanical properties, the porosity in the FDM print parts also negatively affects their sealing functionality. With several experimental results, it can be observed that these parts exhibit poor sealing of liquids and gases, which restrict their usage in sealing applications. The other defect in FDM processed prints is the surface roughness on the part. The side-by-side line effect and the staircase effect that happen due to layer-by-layer deposition cause the surface roughness. This scenario is prominent in inclined and curved surfaces. Figure 13 a–c indicates the surface roughness of Nylon, ABS and PLA printed using the FDM process. Because of the line effect that has occurred during the filament deposition, the finished surface of these parts tends to be rough. From Figure 13-d, it is clearly visible that due to the layer arrangement process, the staircase effect is prominent in curved structures. This is noted as one of the drawbacks in FDM printed parts when compared with the surface finish of parts created by milling or molding [24, 25].

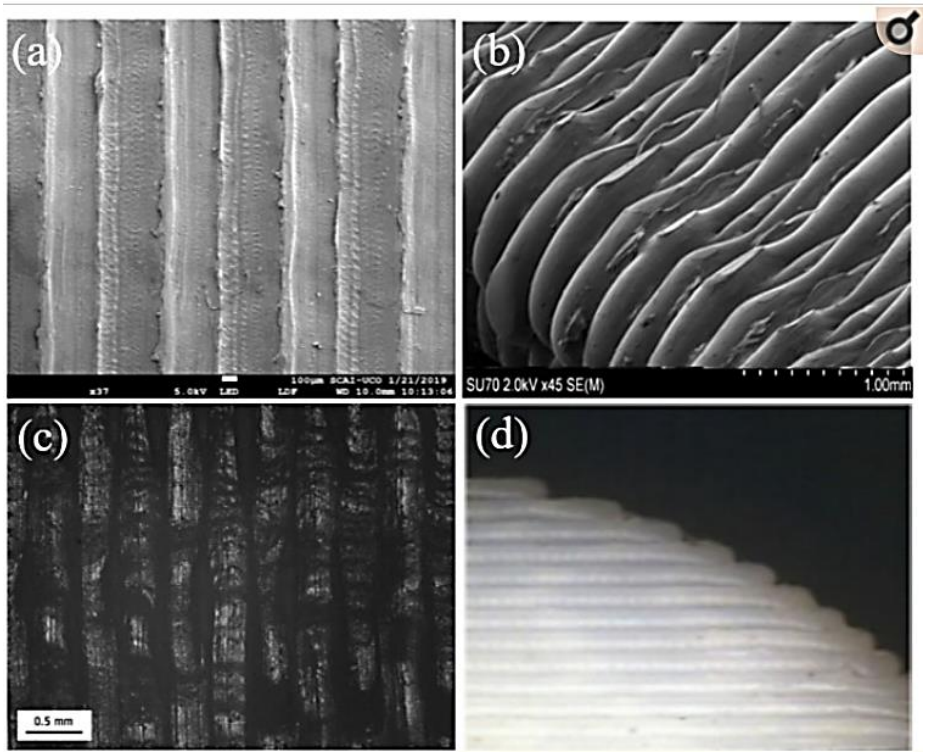

Figure 13: (**a**) Surface roughness of the Nylon FDM specimen. (**b**) Surface roughness of the ABS FDM specimen. (**c)** Surface roughness of the PLA FDM specimen. (**d**) Staircase effect in the FDM printed curved surfaces [26].

One more predominant imperfection in the FDM process is the internal stress buildup in the part during printing, because of fast warming and cooling cycles. This causes non-uniform temperature angles, and the subsequent remaining pressure prompts shape distortion. Rapid cooling empowers the deposited layer to solidify rapidly. At the point when a recently expelled fiber gets saved on the solidified layer, it creates a nearby re-melting affect, guaranteeing the connection between hardened layer and the fiber. This outcomes in uneven heating and cooling, which produce non-uniform temperature gradients. Because of this non-uniform temperature inclination, uneven pressure develops in both the recently kept layer and the recently deposited layer. These burdens influence the shape and aspects of the last parts. There are various kinds of distortions, like cross over or longitudinal shrinkage, bucking, twisting, or angular distortion. This shrinkage causes delamination of layers and distorting, where the part becomes bended from the corners and unsticks from the printing bed. The shape distortion can be limited by utilizing the ideal nozzle temperature, a slower printing speed, a 45° raster angle and increased layer thickness. The most

widely recognized strategy to avoid distortion is applying an adhesive to the printing bed so the part sits firmly on the stage without unsticking. Setting unpleasant borosil glass on the printing bed, applying Kapton tape, which is produced using polyamide film and silicone glue, treating the printing bed with polyvinyl acetic acid derivation (PVA)- based mixtures, encasing the printer with a protection packaging, decreasing the infill and designing the base layer of the part so it can make up for the pressure are a portion of the normal practices to limit the wrapping. Various methods are in practice to minimize these drawbacks. They can be applied before printing or after the printing [27,28].

3.3: Defects observed after the Heat Treatment Process:

One of the most popular methods used to enhance the strength and surface quality of the FDM print parts is heat treatment or thermal annealing. This is a post-processing on complete prints where many investigations have been conducted to understand the effect of this process on the mechanical properties of polymers and composites. With several research works, it has been identified that thermal annealing increases the interlaminar toughness of polymers, making their performance better than injection molding samples. Singh et al. found that when the ABS print part was treated with heat, the surface roughness value and staircase effect were significantly reduced. As the density of the part increased due to the heat, the gaps between layers filled, causing a smoother surface. SEM images show that the bonding between rasters was improved due to annealing. When the annealed temperature reached the glass transition temperature, ABS began to melt slightly. Due to the viscosity reduction at the glass transition temperature, the molecular surface tension was minimized, causing the ABS material to flow on the surface. The reflow of the material filled the porous areas, gaps and staircase effect within layers, resulting in a smoother surface finish and better mechanical properties. When the temperature increased from 105–125 °C, the tensile, flexural and impact strengths also increased, but the results of those mechanical properties were almost similar when the treatment time was increased from 20–30 min. It was, hence, confirmed that the annealing temperature had a huge impact on the final outcome, while the time duration of annealing was insignificant.[29]

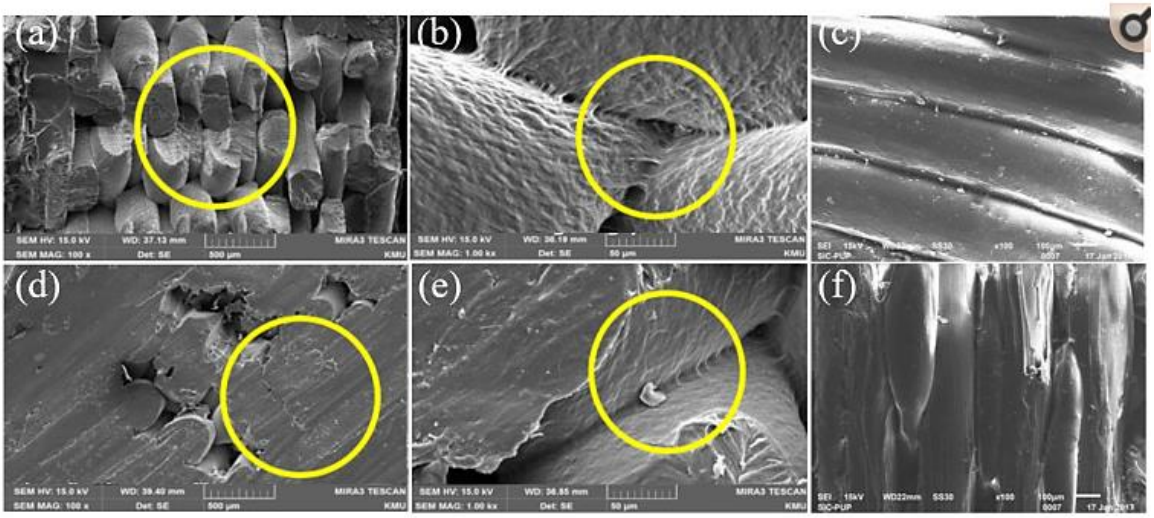

Figure 14: (**a)** Fracture surface of the untreated PLA specimen. (**b**) Bond between PLA filaments of the untreated specimen. (**c**) Surface of the untreated ABS specimen. (**d**) Fracture surface of the annealed PLA specimen. (**e**) Bond between PLA filaments of the annealed specimen. (**f**) Surface of the annealed ABS specimen. Heat treated specimens increased their layer and raster direction [30].

Several experiments have been conducted on PLA printed parts, as PLA is one of the most used polymers in FDM. As per Hong et al. work, it was noted that the mechanical properties including flexural strength and compressive strength were increased due to heat annealing. The bonds between the layers became much stronger with higher temperatures and longer exposure, whereas a sample treated at 140 °C for 600 s showed the maximum bond between layers. The part a and b of the figure 14 above shows the fracture surface and bond between filaments in an untreated PLA specimen, while the d and e part show the fracture surface and bond between filaments in an annealed PLA specimen. From those images, it is clearly visible that heat treatment enhanced the bond between rasters and layers. Even though higher temperatures enhanced the strength of the part, the ductility was drastically reduced. Hence, it is advised to treat the sample with a low heat level to preserve the ductility while enhancing the strength.

Akhoundi et al.'s study indicated several improvements in the printed structure of PLA after thermal annealing. XRD (X-ray diffraction) confirmed that once the PLA samples were annealed, the amorphous areas became semicrystalline. Microscopic analysis showed improved bonding between rasters and layers, as well as no visible voids in the microstructure. Wach et al. noted that

at higher temperatures, the crystallites of PLA grew smaller, while at lower temperatures, the crystallites were much bigger. In both scenarios, the flexural properties exhibited similar results. Hence, it was confirmed that the flexural strength could be increased up to 11%–17% even by keeping the part in a DSC (Differential scanning calorimetry) furnace at a 95 °C for 15 min. Some other methods have also been developed by researchers to overcome the drawbacks in FDM print parts. It includes the use of chemical solutions, laser and ultrasound to enhance the properties of those printed parts [31,32].

CHAPTER 4: METHODOLOGY

4.1: Sample Dimensions:

First of all, the standard specimen size was selected for Charpy impact testing according to ASTM A370 for the printing of our samples. The sample has a notch machined across one of the larger dimensions.

4.2: Design of the Sample:

The specimens for this experiment were printed with fused deposition modelling (FDM) method with PLA and ABS filament as the printing material. The specimens were modelled with Creo parametric 6.0 which is a Computer Aided Design (CAD) software. The test sample dimensions are shown in figure 15.

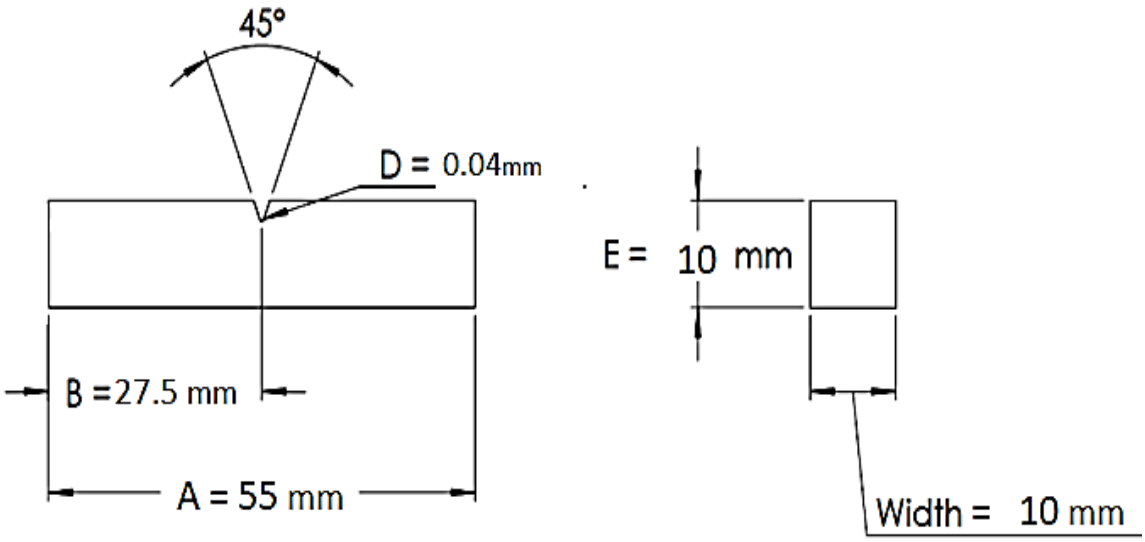

Figure 15: Test Specimen dimensions

This model was later exported as a Standard Tessellation Language (STL) file in Ultimate Cura software which is used at the time of printing the samples. It is a user friendly software having many options to modify the STL file that is imported in it.

S

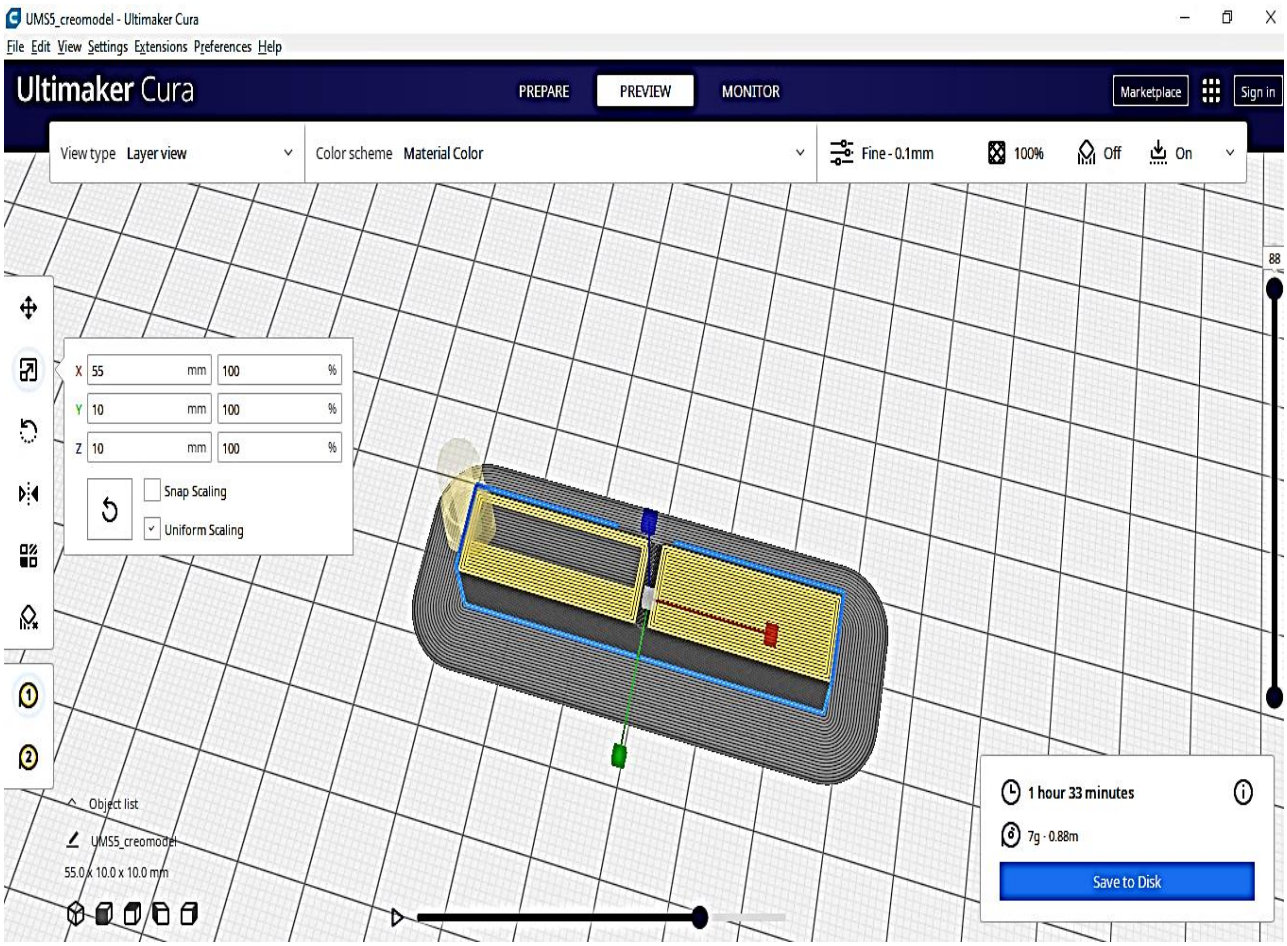

Figure 15(a): Screen shot of Ultimate CURA software showing internal view of STL file of Impact specimen.

4.3: Sample Printing and Build Orientation:

The next step was the selection of the parameters. Raster Angle 0°, 45°, 60°/30°, 90° were used and the build orientation was horizontal as shown in figure 16.

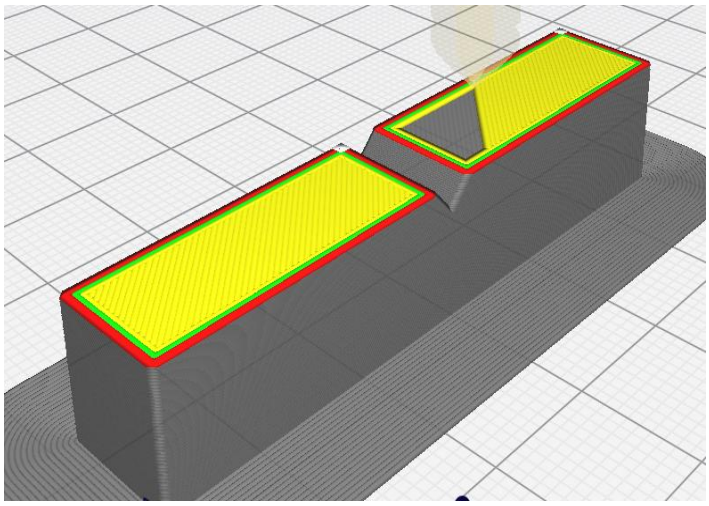

Figure 16: CAD model at raster angle 45 with horizontal build orientation

One sample on raster angle 45° was printed with vertical build orientation as shown in figure 17.

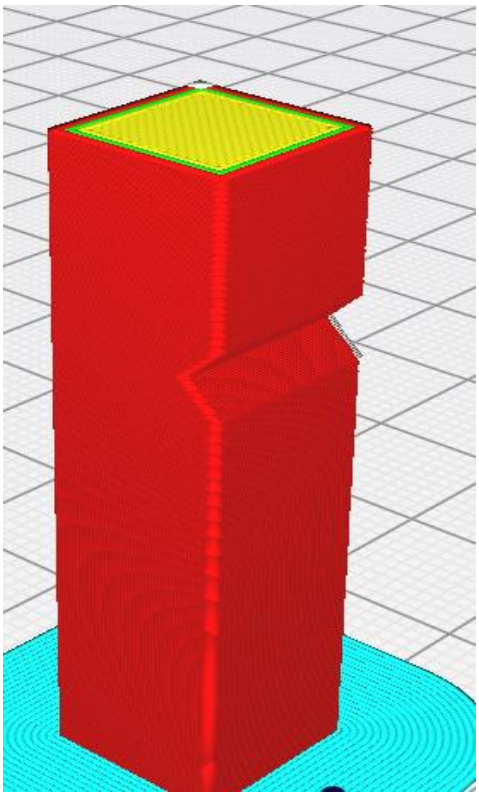

Figure 17: CAD model in vertical orientation and raster angle 45

4.4: Sample ID:

The following table shows the sample id of the printed samples. The sample id provides the information about the raster angle and build orientation of the sample.

Table 3: Samples IDs of Printed Parts

Sample ID	Raster Angle	Build Orientation
0/H	0°	Horizontal
30/H	30°	Horizontal
45/H	45°	Horizontal
90/H	90°	Horizontal
45/V	45°	Vertical

0/H: Fibers in a single layer are printed at the angle of 0° in horizontal direction.

30/H: Fibers in a single layer are printed at the angle of 30° in horizontal direction.

45/H: Fibers in a single layer are printed at the angle of 45° in horizontal direction.

90/H: Fibers in a single layer are printed at the angle of 90° in horizontal direction.

45/V: Fibers in a single layer are printed at the angle of 45° in vertical direction.

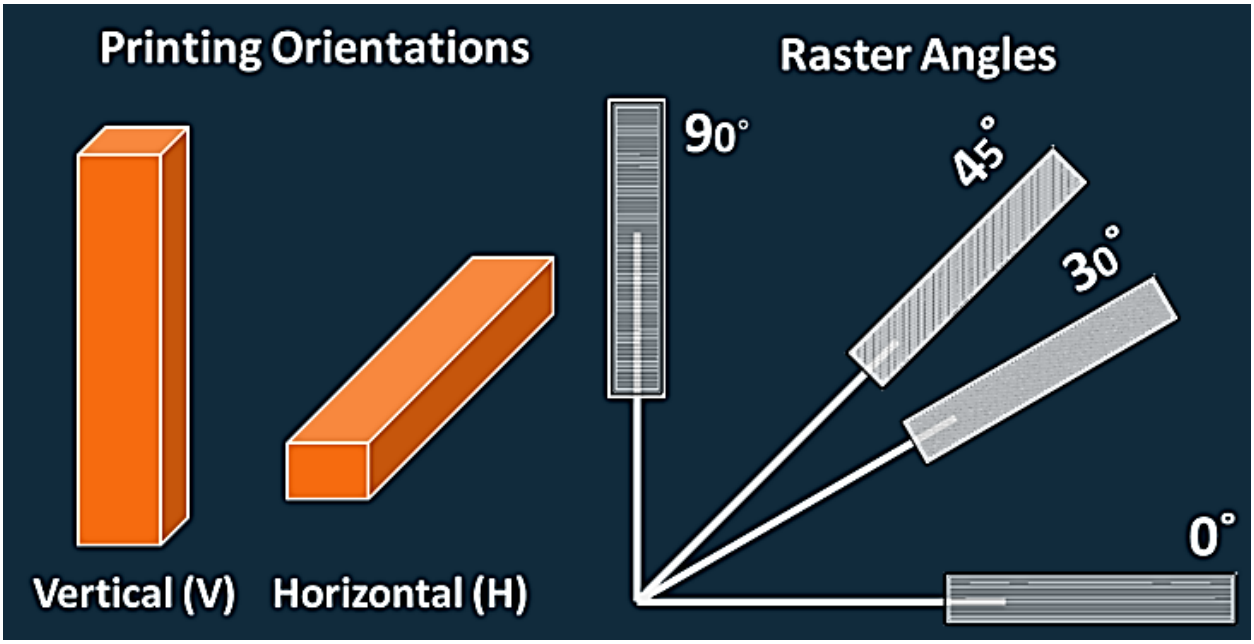

4.5: Print Settings:

The following print settings were used in the Ultimate CURA software for the printing of PLA and ABS samples.

Table 4: Print parameters used for printing in CURA software

Layer height	Layer height	0.1mm
	First layer height	0.2mm
Shells	Top/Bottom Thickness	0.6mm
	Top/Bottom Line Directions	Horizontal:[0]/[45]/ [60]/[90] Vertical: [45]
	Wall Thickness	0.8mm
Infill	Fill density	100%
	Fill pattern	Grid
	Infill Overlap Percentage	0%
Speed	Print speed	50mm/s
	Travel speed	100mm/s
Temperature	Extruder	210ºC for PLA 240ºC for ABS
	Build plate	60ºC for PLA 110ºC for ABS

4.6: Impact Testing:

After the printing of the samples, Charpy Impact testing was performed on the apparatus shown in figure 19. Charpy impact testing is used to determine the amount of energy absorbed by a material during fracture. In this test the notches specimen is fixed on one end of the apparatus. The pendulum swings through during the test and the height of the pendulum gives the energy absorbed during the fracturing of the specimen. The amount of energy absorbed is known as the impact energy and its units are joules. This test shows weather a material is ductile or brittle. The appearance of the Fracture surface also give information about the type of fracture that has occurred. The schematic for the Charpy impact test is shown in figure 18:

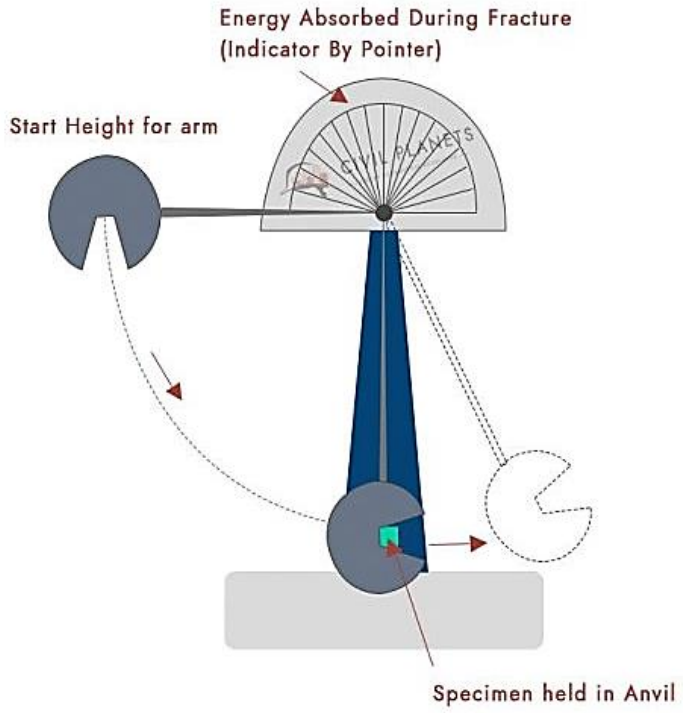

Figure 18: Schematic diagram of Charpy Impact test Apparatus

The procedure for the Charpy Impact test is as follows:

- First of all lift the pendulum to the starting position to check whether the machine is adjusted correctly.
- After calibration, the test specimen is placed correctly by using the centering point on the machine.
- Then turn the pointer needle to the end value and release the pendulum.

- The pendulum swings down and the cuts the specimen in two parts.
- Due to the energy absorbed by the specimen, the pendulum will not reach the maximum top position on the other side.
- The energy in joules is noted from the position of the pointer needle.

Figure 19: Charpy Impact Test Apparatus used for Impact Testing of the samples

The impact energy is expressed in joules. Impact strength is calculated by dividing energy in joules by the area under the notch.

Impact Strength = Impact Energy / Area of the Fracture

4.7: Heat Treatment Process:

Some of the 3d printed samples were impact tested while others were subjected to heat treatment. Heat treatment process is carried out in a mini CVD tube furnace which is a controlled temperature furnace.

Figure 20: Mini CVD Tube furnace used for heat treatment

The maximum temperature this tube furnace can heat the specimen is 1100ºC. The samples were heated 35ºC to 40ºC above the glass transition temperature. For PLA, as the glass transition temperature is 60°C, the samples were heated at 100ºC for 1 hour. Similarly, ABS was heated for 1 hour at a temperature of 150ºC. Different heating temperatures were tested but the maximum impact strength came from heating the PLA and ABS samples at 100ºC and 150ºC respectively. The samples were placed in a die made of aluminum and after the heat treatment the samples were air cooled.

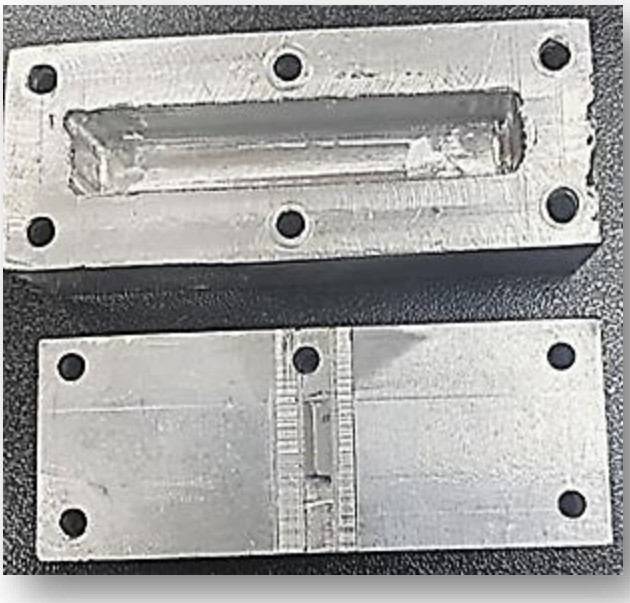

Figure 21: Aluminum Die to enclose the samples during heat treatment

The heat treatment cycle which shows the complete heat treatment process, the time and temperature at which the parts are heated. Also, the cooling process used after the heat treatment is also shown.

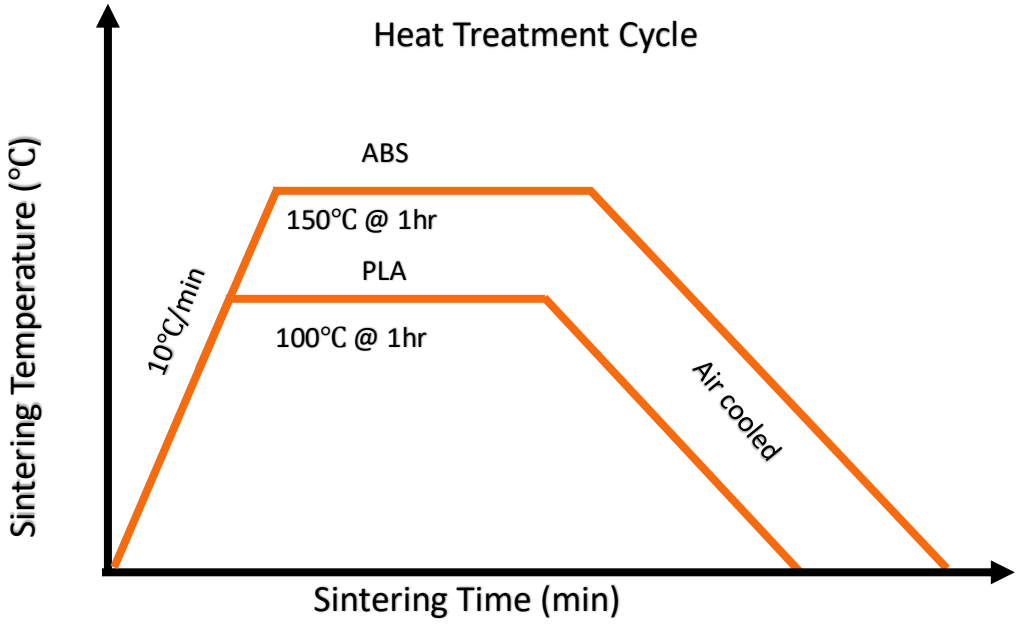

Figure 22: Heat Treatment Cycle of the 3D printed samples

4.8: Scanning Electron Microscope (SEM):

Scanning electron microscope provides information about the surface of any sample. The sample must have the ability to withstand the vacuum created in the chamber and the bombardment of the electrons. SEM enables looking at the connection between electrons produced by the source at the highest point of the section, advanced toward the sample, and the molecules that make up the sample. These electrons communicate with the surface of the sample to deliver signals gathered by the detector that gives an image. 3D printed parts require accurate images and any faults that may compromise the reliability of the part. SEM is a tool which can give structural information to improve the quality of the final product. An advantage is that it gives chemical composition of the particle. In this project, the samples that are impact tested both with and without heat treatment are observed in Scanning electron microscope. The images of the samples at different raster angles are shown below:

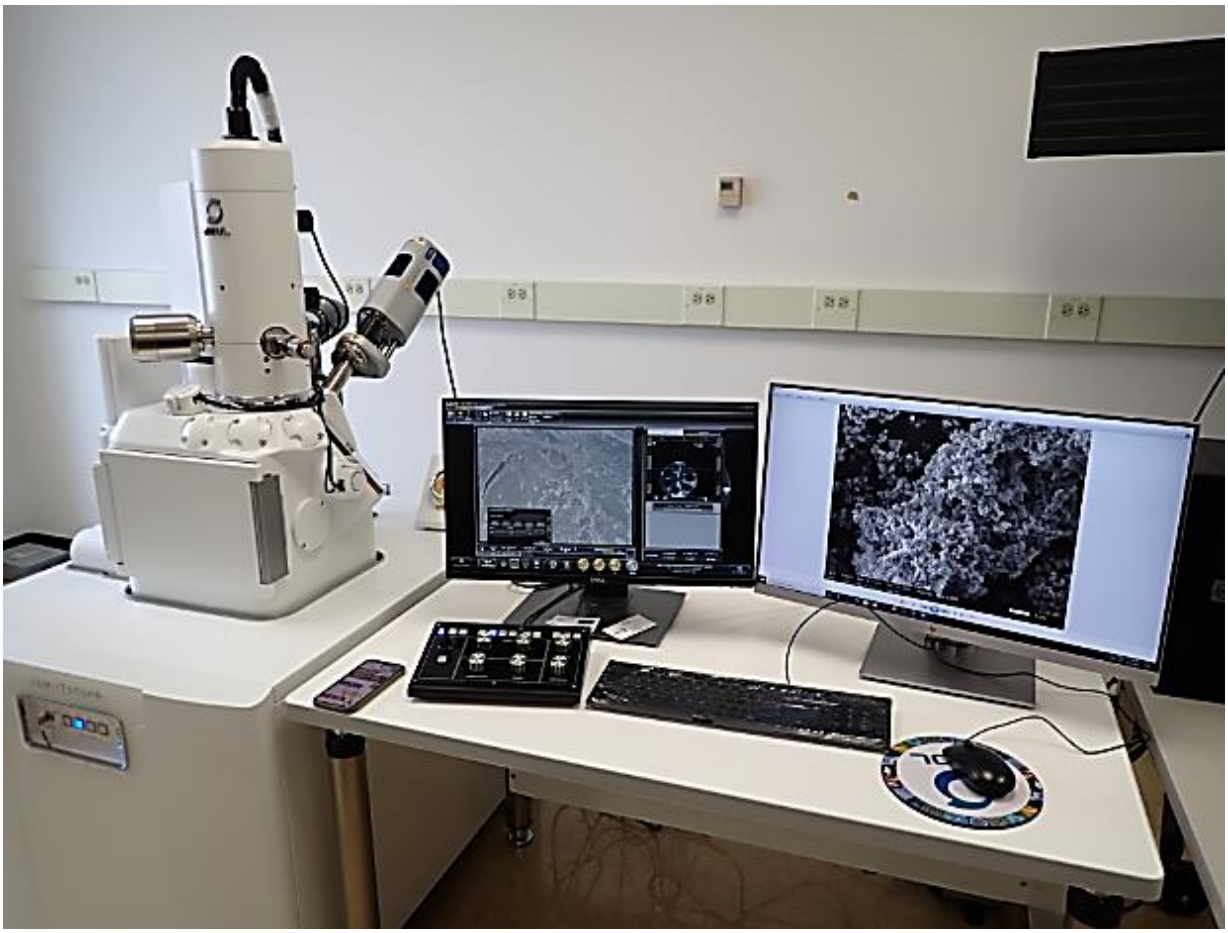

Figure 23: Scanning Electron Microscope used to examine the fractured surfaces

CHAPTER 5: RESULTS AND DISCUSSIONS

5.1: Cracks propagation:

Following two figures show the crack propagation in the fractured samples. The crack starts from the notch location and propagated towards the impact zone.

5.1.1: Samples without Heat Treatment:

In samples which are impact tested before the heat treatment, the crack is propagated in a fairly linear manner. This is because of interlayer porosity and weak adhesion between the layers. These samples absorb less energy before fracturing causing flat fracture as shown in figure 24.

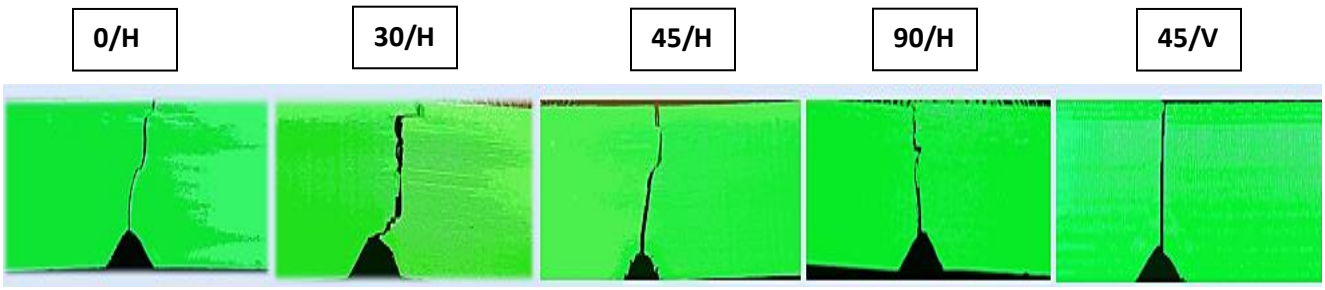

Figure 24: Crack Propagation in samples before heat treatment

5.1.2: Samples with Heat Treatment

Crack Propagation in Samples without heat treatment is shown in figure 25. In heat treatment samples the crack is more distorted. It is due to heat treatment that the interlayer bonding is enhanced. Thus the samples absorb more energy before fracturing.

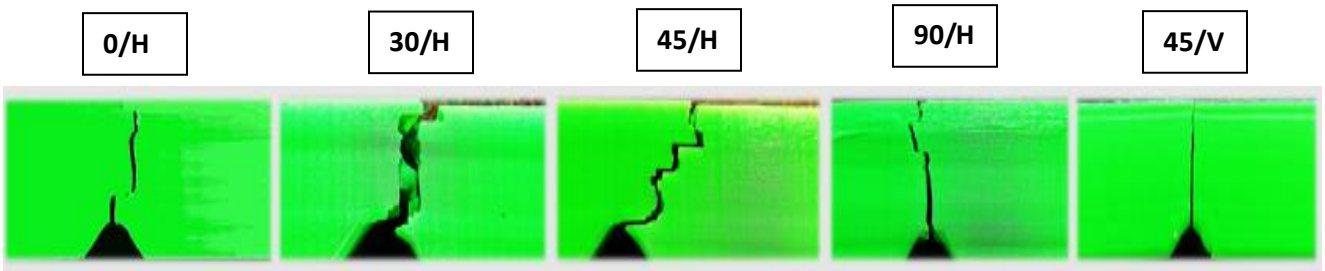

Figure 25: Crack Propagation in samples after heat treatment

5.2: Impact Test Before Heat Treatment:

To determine the impact strength of the samples, Charpy impact test was performed before the heat treatment process. For PLA, In horizontal build orientation raster angles 0°, 30°, 45° and 90° are impact tested and their impact energy is noted from the movement of the pointer needle. In vertical orientation raster angle 45° is tested and energy is noted down. Impact Strength is calculated by the following formula:

$$\text{Impact Strength} = \text{Impact Energy} / \text{Area of the Fracture}$$

Area of the fracture surface for all the sample will be same. It is calculated by the product of the length and width at the fracture surface. Length of the sample is 10 mm but 2 mm is the nozzle length. So, the length of the fracture surface will be 8 mm. Width is 10 mm.

$$\text{Area of the fracture surface} = (\text{Length of the fracture}) * (\text{Width of the fracture})$$

$$= (8\ \text{mm}) * (10\ \text{mm})$$

$$= 80\ \text{mm}^2$$

Impact Energy is calculated in Joules. Thus, the impact strength will be:

$$\text{Impact Strength} = (\text{Impact Energy in joules}) / (80\ \text{mm}^2)$$

Table 5 shows the results of the impact tests performed on PLA samples. The values given in the table are the impact strengths and their unit is kJ/m^2.

Table 5: Impact strength of PLA before Heat treatment

Impact Strength of PLA Before Heat-treatment	
Sample ID	**Impact Strength (kJ/m^2)**
0/H	23.12
30/H	23.75
45/H	25.00
90/H	26.25
45/V	22.50

Figure 26 shows the bar chart for the PLA samples as they are printed and impact tested on the Charpy impact test apparatus.

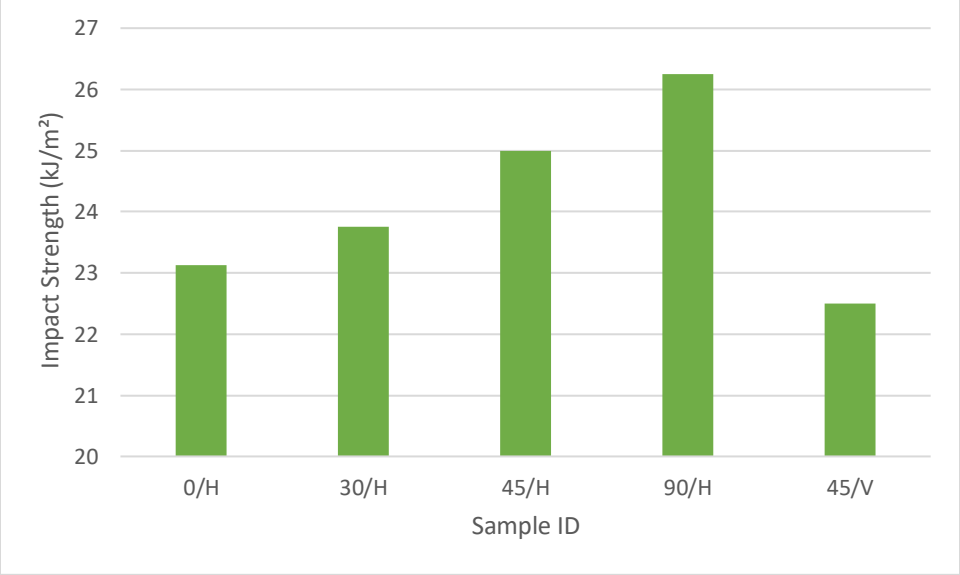

Figure 26: Impact Strength of PLA without heat treatment

For the ABS samples, In vertical orientation raster angle 45° is tested while in horizontal build orientation raster angles0°, 45°, 60° and 90° are tested on the Charpy impact test apparatus and results are noted. Table 6 shows the impact test results of ABS samples.

Table 6: Impact strength of ABS before Heat treatment

Impact Strength of ABS Before Heat-treatment	
Sample ID	**Impact Strength (kJ/m^2)**
0/H	21.00
45/H	24.00
60/H	27.00
90/H	27.50
45/V	18.75

Figure 27 shows the bar chart for the ABS samples as they are printed and impact tested on the Charpy impact test apparatus.

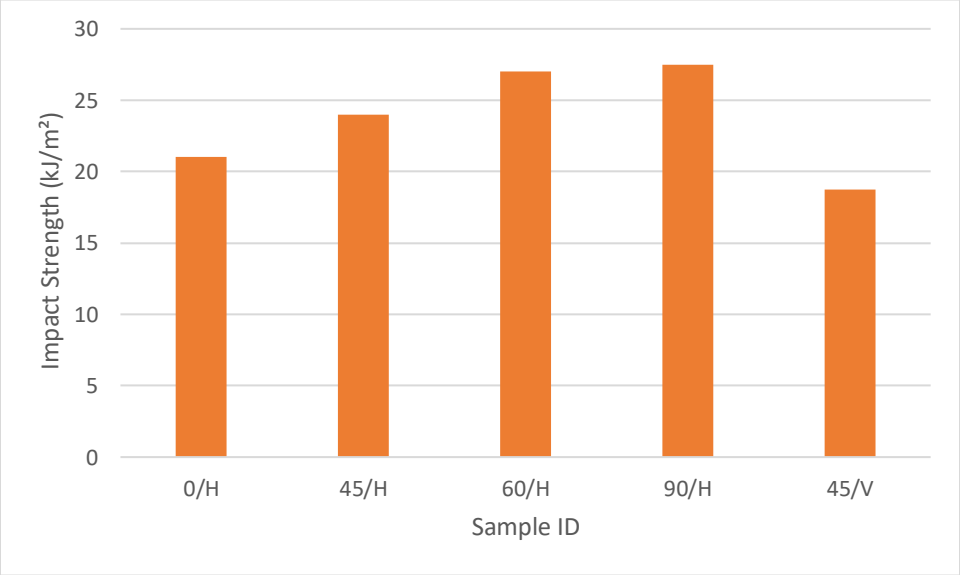

Figure 27: Impact Strength of ABS without heat treatment

5.3: Impact Test After Heat Treatment:

Heat treatment of the remaining PLA samples is done at 100°C for 1 hour. After the heat treatment the PLA parts are again impact tested to note the effect of heat treatment on the impact strength. The impact testing shows that with heat treatment the impact strength is increased.

Table 7: Impact strength of PLA after heat treatment

Impact Strength of PLA After Heat-treatment	
Sample ID	**Impact Strength (kJ/m^2)**
0/H	25.00
30/H	24.37
45/H	26.00
90/H	27.00
45/V	23.00

The results mentioned in the table are shown in the bar chart below:

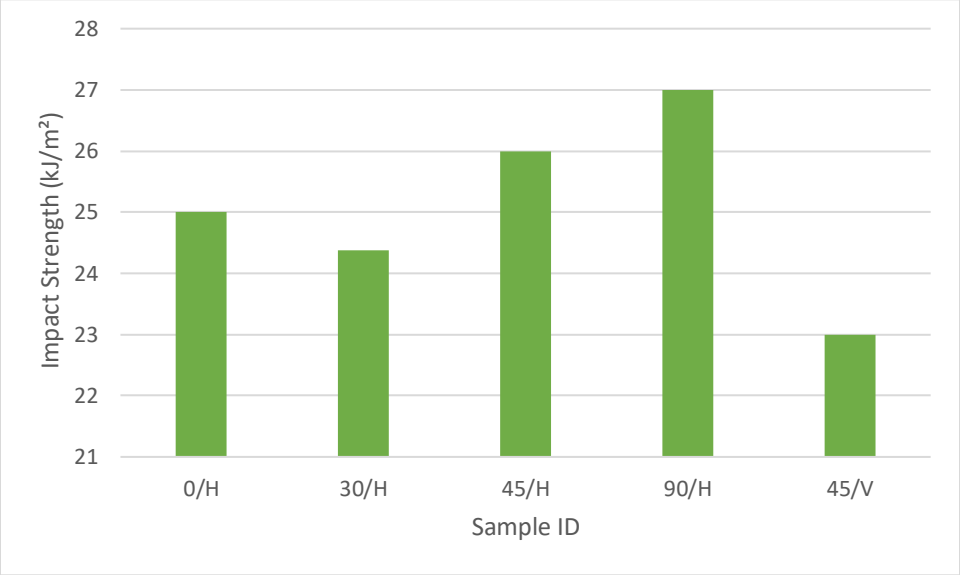

Figure 28: Impact Strength of PLA with heat treatment

ABS samples are heat treated at 150°C for 1 hour and then Charpy impact test is performed to check whether the heat treatment has positive or negative effect on the impact properties. The impact testing shows that with heat treatment the impact strength for ABS is significantly increased.

Table 8: Impact strength of ABS after heat treatment

Impact Strength of ABS After Heat-treatment	
Sample ID	**Impact Strength (kJ/m^2)**
0/H	40.00
45/H	53.75
60/H	75.00
90/H	76.25
45/V	26.25

Figure 29 shows the bar chart for the ABS samples after heat treatment and impact tested on the Charpy impact test apparatus.

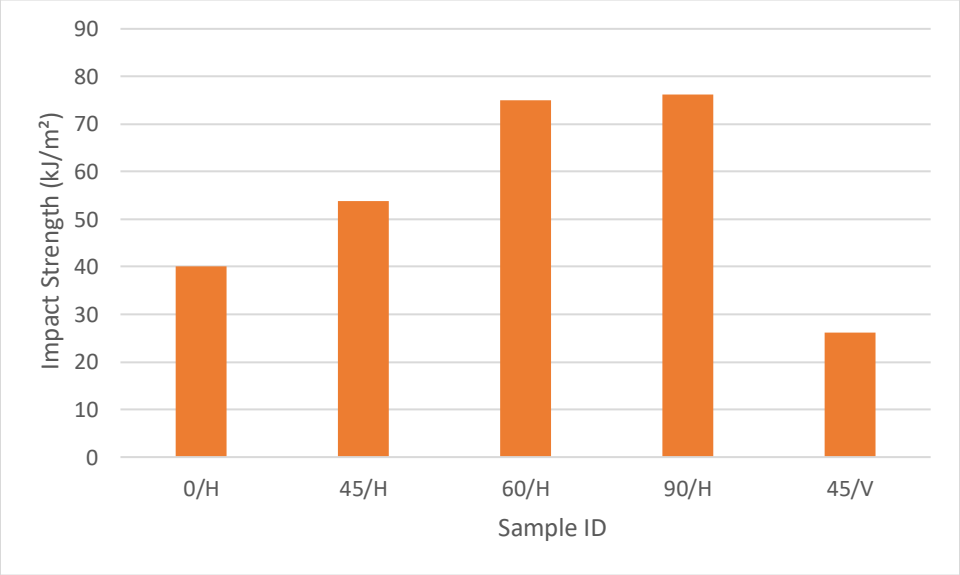

Figure 29: Impact Strength of ABS with heat treatment

The combined results for the PLA samples both with and without heat treatment are given in the following table.

Table 9: Impact strength of PLA before and after heat treatment

Impact Strength of PLA with & without Heat Treatment		
Sample ID	**Impact Strength As Printed**	**Impact Strength Heat Treated**
0/H	23.12	25.00
30/H	23.75	24.37
45/H	25.00	26.00
90/H	26.25	27.00
45/V	22.50	23.00

The following bar chart shows the impact strength comparison of PLA samples before and after the heat treatment.

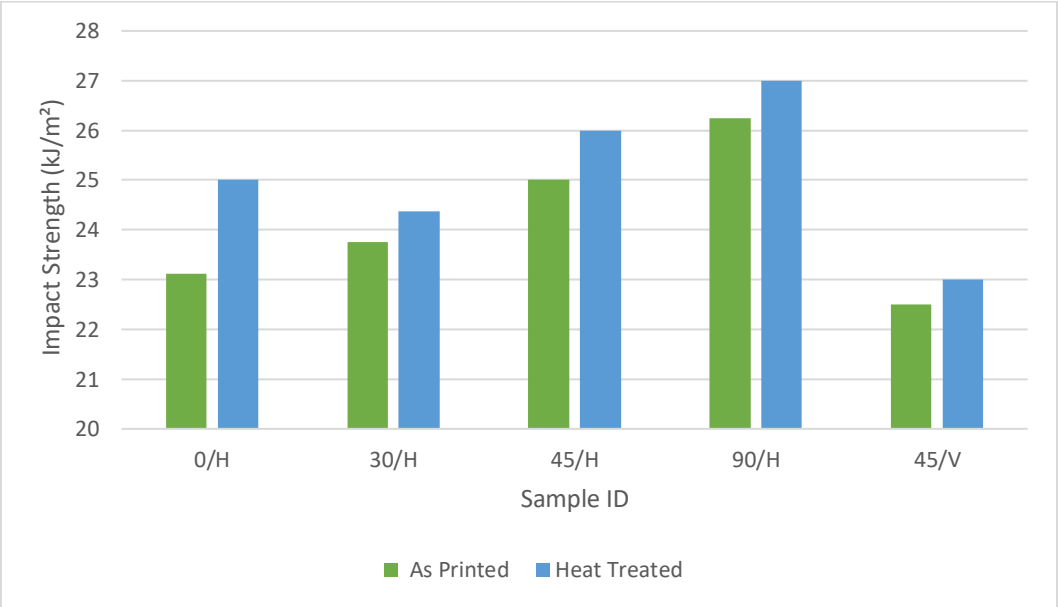

Figure 30: Impact Strength of PLA with and without heat treatment

The combined results for the ABS samples both with and without heat treatment are given in the following table.

Table 10: Impact strength of ABS before and after heat treatment

Impact Strength of ABS with and without Heat Treatment		
Sample ID	**Impact Strength As Printed**	**Impact Strength Heat Treated**
0/H	21.00	40.00
45/H	24.00	53.75
60/H	27.00	75.00
90/H	27.50	76.25
45/V	18.75	26.25

The following bar chart shows the impact strength comparison of PLA samples before and after the heat treatment.

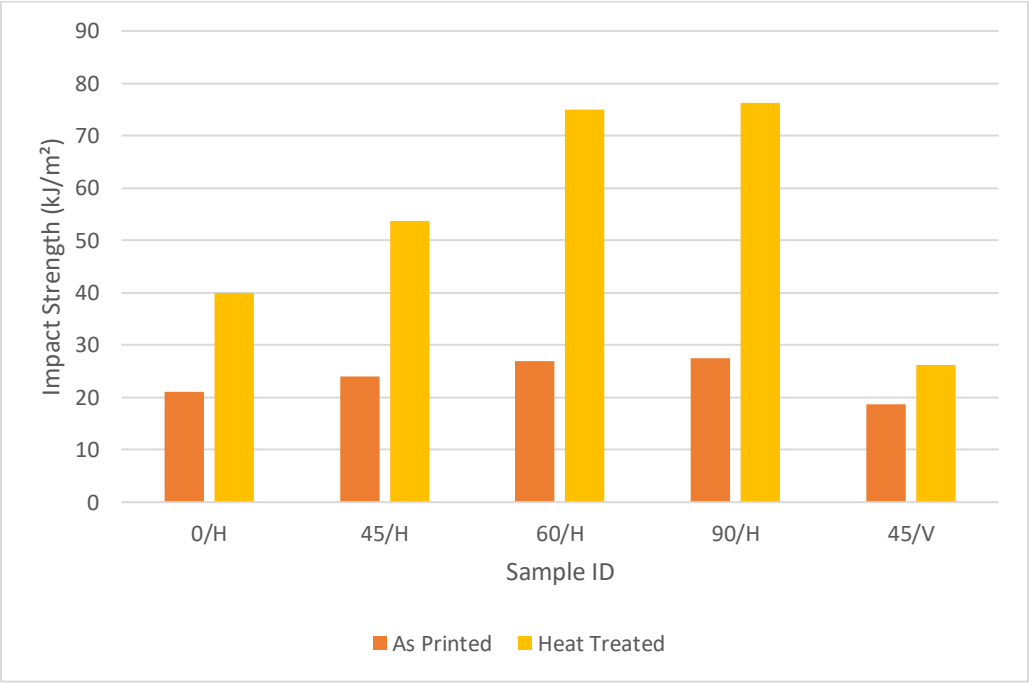

Figure 31: Impact Strength of ABS with and without heat treatment

5.4: Discussion:

It can be observed from the tables that the impact strength is increased by increasing the raster angles, at 0° the impact strength is lowest and at 90° the impact strength is the highest. This is due to the reason that during the printing of the samples, one fiber in each layer of 0° raster angle part, takes more time to complete than that in 90°. Due to this difference of time between the placement of two fibers of a single layer, a temperature difference is created which will cause intralayer distortion.

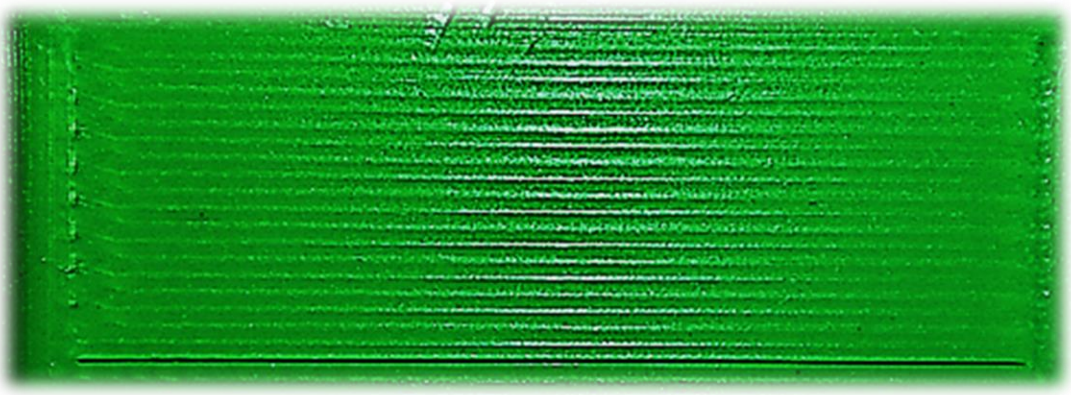

Figure 32: Sample Printed at a raster angle of 0°

It is shown in figure 33 that for 90° raster angle the fibers in each layer are smaller in length so one fiber takes less time to completely print. This results in strong bonding between the fibers of each layer. This makes the part stronger and difficult to break. Due to this reason, Specimen with raster angle 90° absorb more energy than other samples thus its impact strength is the highest.

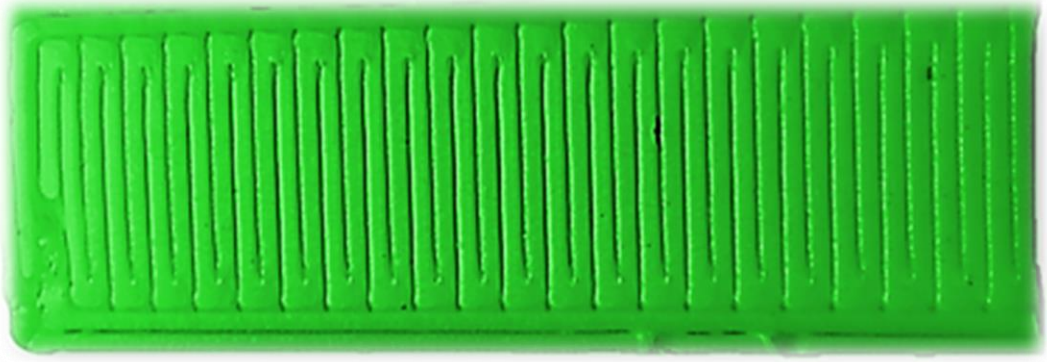

Figure 33: Sample Printed at a raster angle of 90°

For the sample of 45° raster angle in horizontal orientation the impact strength is greater as compared to the 45° in vertical build orientation. This is because of the reason that in vertical 45° the part, when impact tested, is fractured between the layers. This results in low impact strength. Figure 34 shows the fracture surface of 45° raster angle in vertical orientation. The crack is propagated from the upper side to the notch location., it shows that the crack is between two layers and thus the impact strength is less.

Figure 34: Crack propagation in 45V sample

In horizontal 45°, the part is fractured in such a manner that the fibers as well as the layers are cracked by absorbing a greater amount of energy. Figure 35 shows that the fibers as well as the layers break as a result of the impact test. This will take greater amount of energy to break. Thus the impact strength is greater as compared to the sample printed in vertical orientation.

Figure 35: Crack propagation in 45H Sample

5.5: Defects Observed In SEM:

The results of the impact test are shown in table. It is noted that impact strength in horizontal orientation is highest in 90° and lowest in 0°. After the impact test, the samples were observed in the scanning electron microscope to note the fracture surfaces. The main purpose of using SEM was to observe the defects due to which the sample breaks. The failure pattern of different parts printed at 0°, 30°, 45°, 90° are observed. The images show that the surface fractures due to the interlayer distortion, porosity and gaps between the layers.

Figure 36 shows the fracture surface of the ABS sample with raster angle 60° in horizontal build orientation. The notch location and the impact location are labelled. Also the pattern in which the layers are printed is also shown.

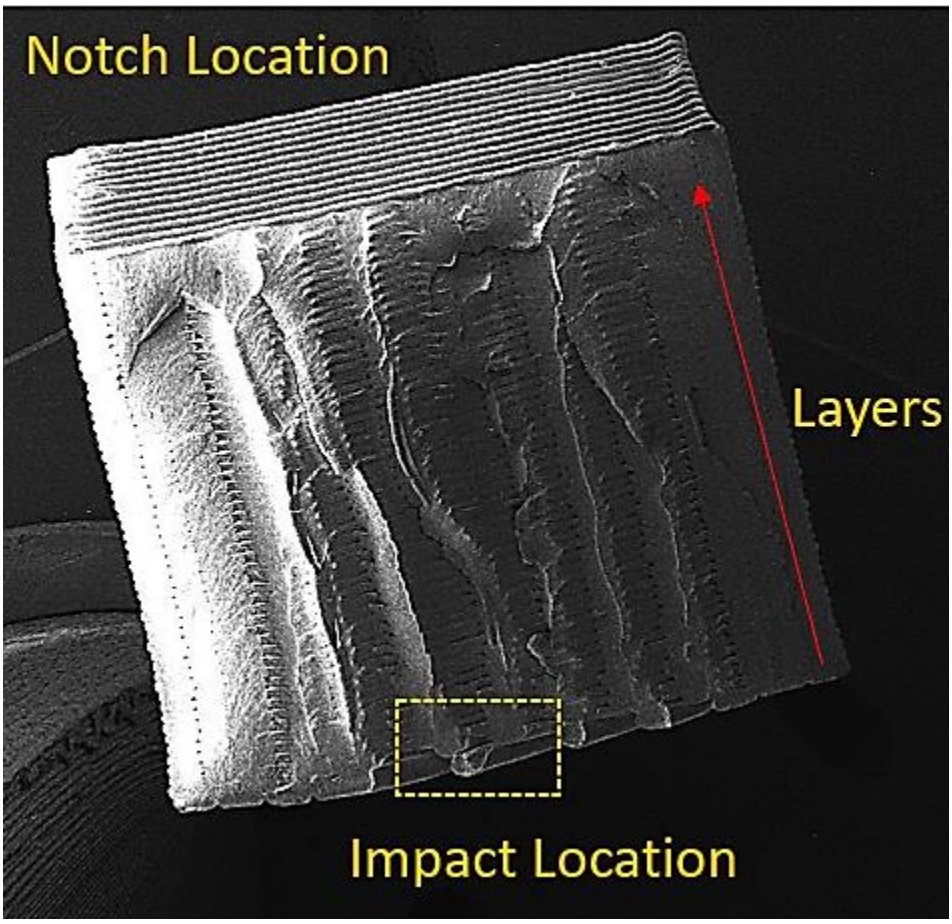

Figure 36: SEM image of the fracture surface at 60 raster angle

It is visible in figure 37 that there is clear lamellar boundary between the fibers. Also the gaps between the layers and the porosity is evident. This shows that there is a difference between the crack propagation between different fibers in the layer. The interlayer porosity in the figure indicated that the adhesion between the subsequent layers is quite low.

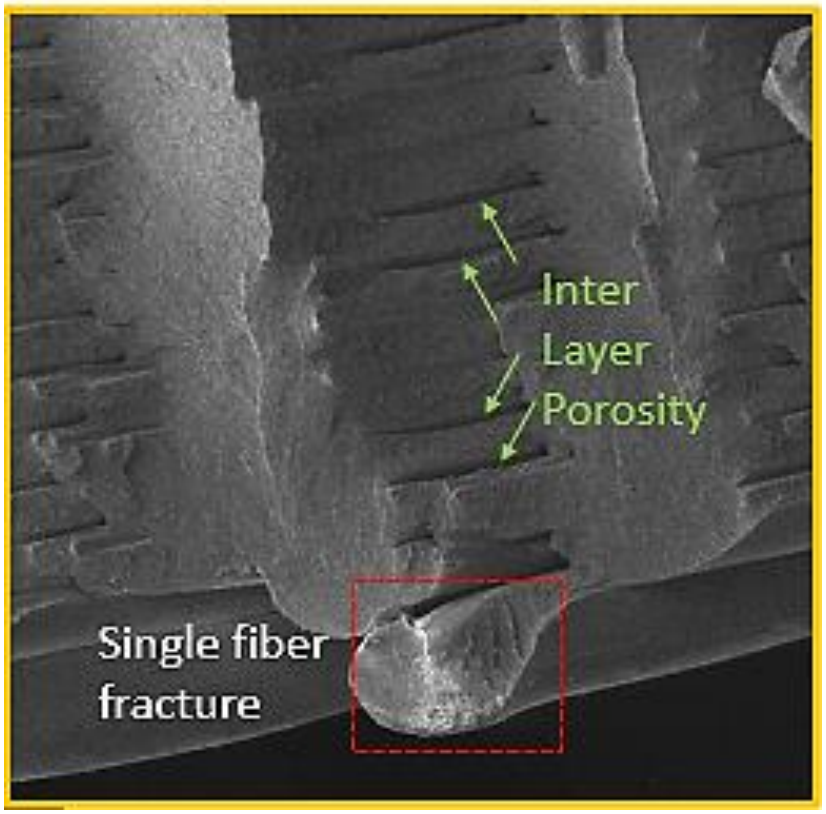

Figure 37: Single fiber structure and porosity in the sample

In figure 38 , the initiation zone of the fracture is visible, Cracks are initiated and propagated along the fracture direction until they reached rapid fracture zone. Parabolic-like feature indicated the growth of a crack in the fiber. In the start of the crack there is plastic deformation as the impact was sudden and large. So the crack initiation shows a distorted shape but as the crack propagates the fracture becomes flat which is called the rapid fracture zone. Rapid Fracture zone having flat appearance is indicative of failure due to overload.

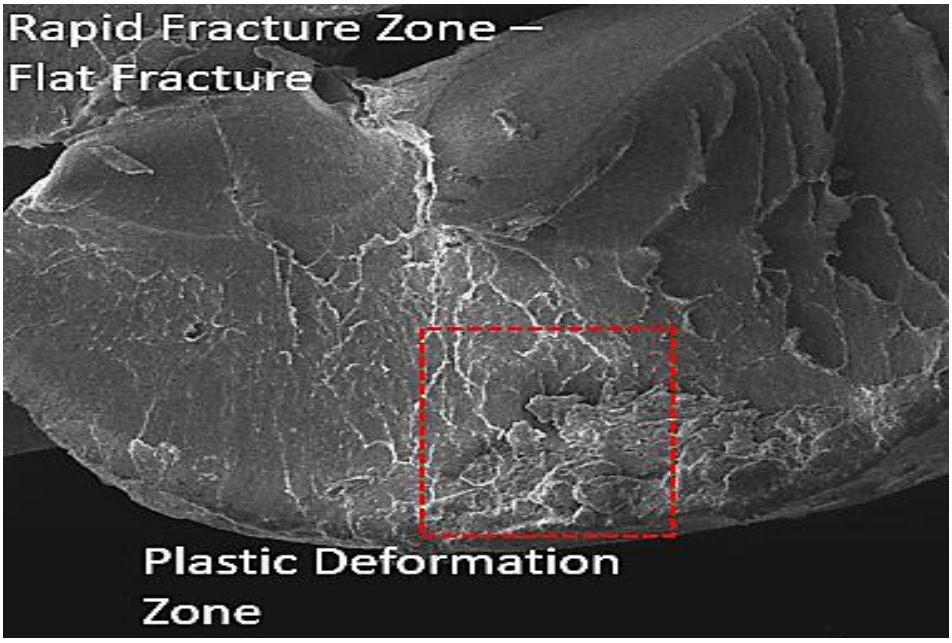

Figure 38: Initiation Zone and propagation of the fracture surface

When the ABS sample at raster angle 60° in horizontal orientation is heated in a controlled temperature furnace for 1 hour at 150°C then the porosity between the layers is reduced. This is due to the reason that during heat treatment the material is fused into the gaps and voids between the layers. Figure 39 shows the crack direction and the interlayer adhesion which is greatly enhanced due to the heat treatment at a temperature above the glass transition temperature.

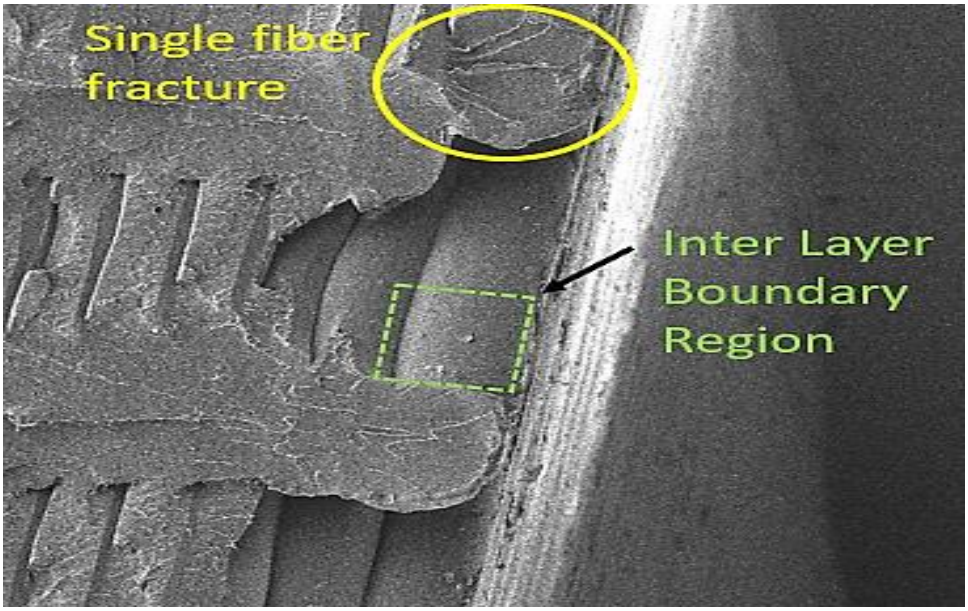

Figure 39: Crack direction in Heat treated sample of 60 raster angle

In figure 40, it is shown that the crack at the start and end of the fiber is flat and plastic deformation is negligible. This is because due to the heat treatment process the bonding between the layers is increased causing the fracture to be flat.

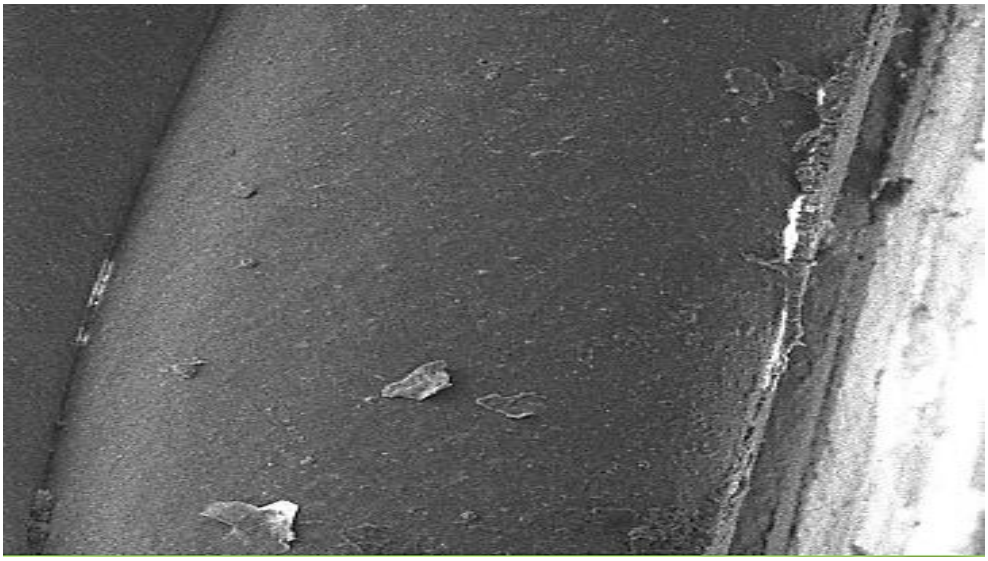

Figure 40: Flat Fracture in the heat treated sample

In case of PLA sample printed at a raster angle of 0° in horizontal build orientation, the impact and notch location are shown in figure 41. The gap between the layers is shown which is the major defect in the printing of this part.

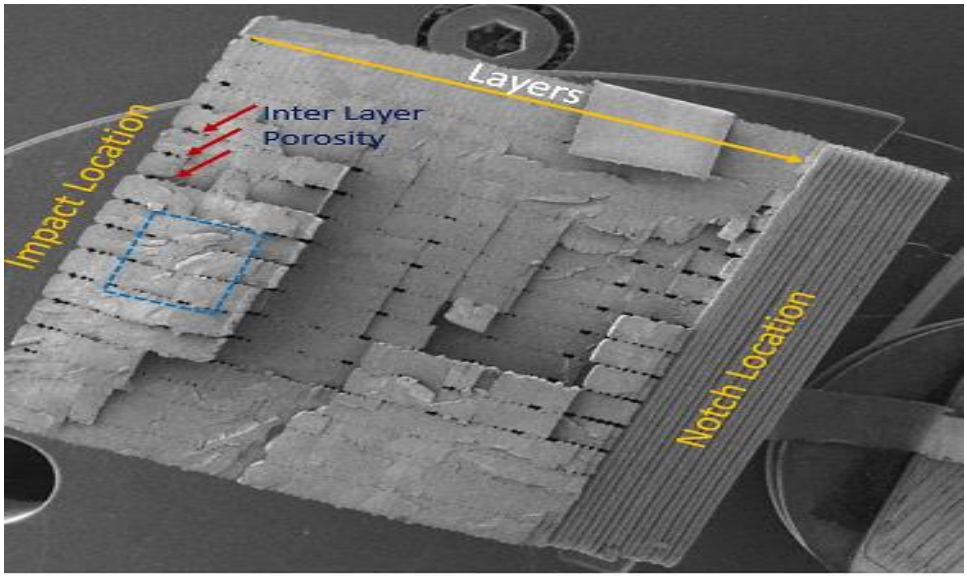

Figure 41: Fracture surface of PLA with raster angle 0

In figure 42, the interlayer porosity is clearly visible. Due to this reason, the crack propagated through the layers is majorly flat. Stratification-like appearance of the fracture surface with a clear lamellar boundary indicates that the crack is smooth without much signs of plastic deformation.

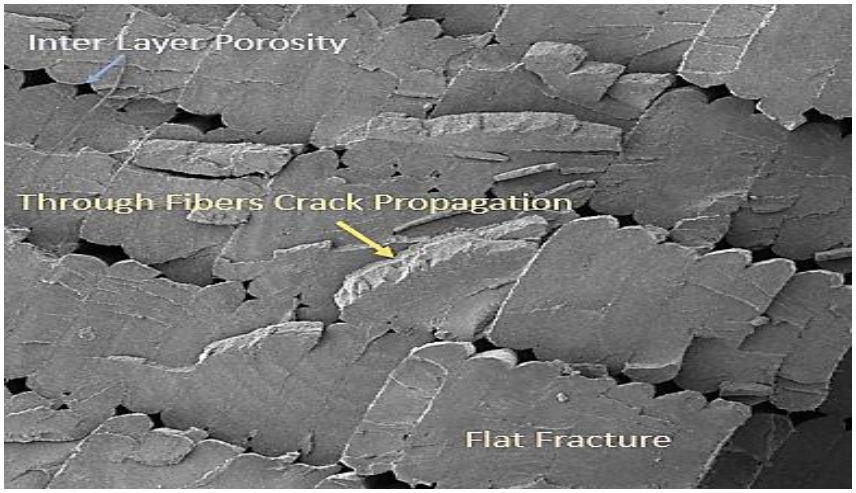

Figure 42: Crack Propagation showing flat fracture and porosity

When the sample at 0° raster angle is heat treated at a temperature greater than the glass transition temperature, the porosity between the layers is somehow reduced. The fracture surface is showing clear signs of plastic deformation this is because of the reason that when the sample is heated the material is fused in the gaps between the layers and the fiber alignment is disturbed. Thus when impact testing of this sample is done the crack propagates through breaking the fibers and shows plastic deformation.

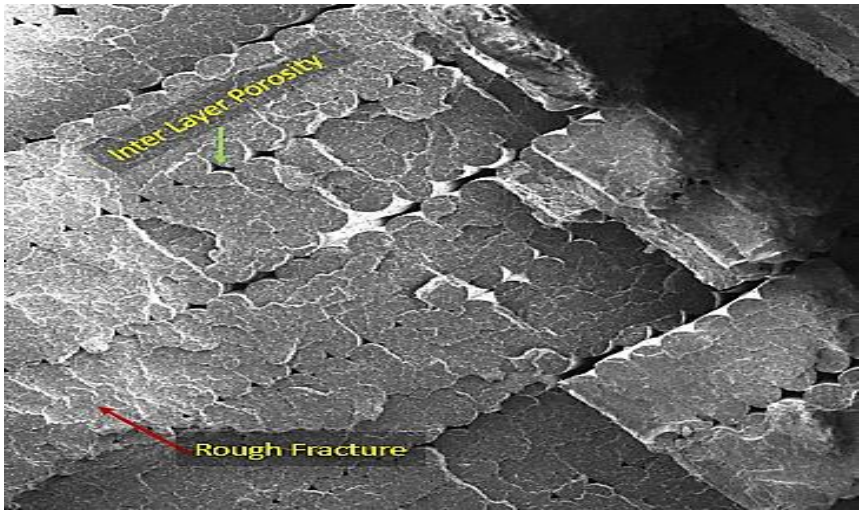

Figure 43: Rough fracture in heat treated PLA sample

CHAPTER 6: CONCLUSION

This study presents an experimental analysis of impact properties of 3D printed samples at different printing parameters and build orientations. Five different raster or printing angles were used to fabricate the 3D printed samples using PLA and ABS material. Impact strength at different printing parameters is analyzed and the optimum parameters are selected for the final printing of the samples. The results that are obtained shows that the effect of printing parameters on the impact strength is great. They have a vital role in the strength of the specimen. Moreover, the fracture in heat treated samples show greater plastic deformations than the samples without heat treatment. The microscopic analysis of the samples in the scanning electron microscope showed interlayer porosity and gaps between the layers. After the heat treatment, the gaps are greatly reduced which would make the sample more impact resistant. This shows that the impact properties increase when the samples are heat treated at a temperature slightly above the glass transition temperature.

Recommendations of Future Research:

The following recommendations for future research are made based on the results of this study:

- The impact strength of PLA and ABS samples can be further studied by varying other printing parameters.
- Other Mechanical properties can also be studied at the same printing conditions used in this study.
- Heat Treatment of the samples with addition of any reinforcing fibers or selective additives.

References:

1. https://markforged.com/resources/blog/pla-abs-nylon
2. https://markforged.com/resources/blog/pla-abs-nylon
3. L. Wang, W.M. Gramlich, D.J. Gardner
   Improving the impact strength of Poly(lactic acid) (PLA) in fused layer modeling
4. J.F.M. Fernandes, M. Leite, L. Reis, A.M. Deus, M.F. Vaz
   Study of the influence of 3D printing parameters on the mechanical properties of PLA
   C.K. Chua, W.Y. Yeong, M.J. Tan, E.J. Liu, S.B. Tor (Eds.), 3rd int. Conf. Prog. Addit. Manuf. (Pro-AM 2018), Nanyang Technological University (2018)
5. J.F.M. Fernandes, M. Leite, L. Reis, A.M. Deus, M.F. Vaz
   Study of the influence of 3D printing parameters on the mechanical properties of PLA
6. J.F.M. Fernandes, M. Leite, L. Reis, A.M. Deus, M.F. Vaz
   Study of the influence of 3D printing parameters on the mechanical properties of PLA
   C.K. Chua, W.Y. Yeong, M.J. Tan, E.J. Liu, S.B. Tor (Eds.), 3rd int. Conf. Prog. Addit. Manuf. (Pro-AM 2018), Nanyang Technological University (2018)
7. J.F.M. Fernandes, M. Leite, L. Reis, A.M. Deus, M.F. Vaz
   Study of the influence of 3D printing parameters on the mechanical properties of PLA
   C.K. Chua, W.Y. Yeong, M.J. Tan, E.J. Liu, S.B. Tor (Eds.), 3rd int. Conf. Prog. Addit. Manuf. (Pro-AM 2018), Nanyang Technological University (2018)
8. U.A. Dar, Y.J. Xu, S.M. Zakir, M. Saeed
   The effect of injection molding process parameters on mechanical and fracture behavior of polycarbonate polymer
   J Appl Polym Sci, 44474 (2017), pp. 1-9
9. Benwood, C., Anstey, A., Andrzejewski, J., Misra, M., & Mohanty, A. K. (2018). Improving the Impact Strength and Heat Resistance of 3D Printed Models: Structure, Property, and Processing Correlation ships during Fused Deposition Modeling (FDM) of Poly (Lactic Acid). ACS Omega,3(4), 4400-4411. doi:10.1021/acsomega.8b00129
10. Algarni, M. The Influence of Raster Angle and Moisture Content on the Mechanical Properties of PLA Parts Produced by Fused Deposition Modeling. Polymers 2021, 13, 237

11. Zhang, X.; Chen, L.; Mulholland, T.; Osswald, T.A. Effects of raster angle on the mechanical properties of PLA and Al/PLA composite part produced by fused deposition modeling. Polym. Adv. Technol. 2019, 30, 2122–2135
12. Fatimatuzahraa, A.; Farahaina, B.; Yusoff, W. The Effect of Employing Different Raster Orientations on the Mechanical Properties and Microstructure of Fused Deposition Modeling Parts. In Proceedings of the 2011 IEEE Symposium on Business, Engineering and Industrial Applications (ISBEIA), Langkawi, Malaysia, 25–28 September 2011; pp. 22–27
13. Rodríguez-Panes, A.; Claver, J.; Camacho, A.M. The Influence of Manufacturing Parameters on the Mechanical Behaviour of PLA and ABS Pieces Manufactured by FDM: A Comparative Analysis. Materials 2018, 11, 1333.
14. Rismalia, M.; Hidajat, S.C.; Permana, I.G.R.; Hadisujoto, B.; Muslimin, M.; Triawan, F. Infill pattern and density effects on the tensile properties of 3D printed PLA material. J. Phys. Conf. Ser. 2019, 1402, 044041
15. Baich, L.; Manogharan, G.; Marie, H. Study of infill print design on production cost-time of 3D printed ABS parts. Int. J. Rapid Manuf. 2015, 5, 308.
16. Abeykoon, C.; Sri-Amphorn, P.; Fernando, A. Optimization of fused deposition modeling parameters for improved PLA and ABS 3D printed structures. Int. J. Light. Mater. Manuf. 2020, 3, 284–297.
17. Guimarães, A.L.A.; Neto, V.G.; Foschini, C.R.; Azambuja, M.D.A.; Hellmeister, L.A.V. Influence of ABS print parameters on a 3D open-source, self-replicable printer. Rapid Prototyp. J. 2020, 26, 1733–1738.
18. Niaounakis, M., Kontou, E., & Xanthis, M. (2010). Effects of aging on the thermomechanical properties of poly (lactic acid). Journal of Applied Polymer Science,119(1), 472-481. https://dx.doi:10.1002/app.32644
19. Makara Lay, Nuur Laila Najwa Thajudin, Zuratul Ain Abdul Hamid, Arjulizan Rusli, Muhammad Khalil Abdullah, Raa Khimi Shuib, Comparison of physical and mechanical properties of PLA, ABS and nylon 6 fabricated using fused deposition modeling and injection molding, Composites Part B: Engineering, Volume 176,2019,107341,ISSN 1359-8368.

20. J. Zhang, K. Tashiro, H. Tsuji, A.J. Domb Disorder-to-Order phase transition and multiple melting behavior of poly(L-lactide) investigated by simultaneous measurements of WAXD and DSC Macromolecules, 41 (2008), pp. 1352-1357
21. (Kumar M., Ramakrishnan R., Omarbekova A. 3D printed polycarbonate reinforced acrylonitrile–butadiene–styrene composites: Composition effects on mechanical properties, micro-structure and void formation study. *J. Mech. Sci. Technol.* 2019;33:5219–5226. doi: 10.1007/s12206-019-1011-9
22. Dong C. Effects of process-induced voids on the properties of fiber-reinforced composites. *J. Mater. Sci. Technol.* 2016;32:597–604. doi: 10.1016/j.jmst.2016.04.011
23. Rodríguez J.F., Thomas J.P., Renaud J.E. Mechanical behavior of acrylonitrile butadiene styrene (ABS) fused deposition materials. Experimental investigation. *Rapid Prototyp. J.* 2001;6:175–186. doi: 10.1108/13552540010337056.
24. He Q., Wang H., Fu K., Ye L. 3D printed continuous CF/PA6 composites: Effect of microscopic voids on mechanical performance. *Compos. Sci. Technol.* 2020;191:108077. doi: 10.1016/j.compscitech.2020.108077
25. Improvement of Surface Roughness and Hydrophobicity in PETG Parts Manufactured via Fused Deposition Modeling (FDM): An Application in 3D Printed Self-Cleaning Parts.Barrios JM, Romero PE Materials (Basel). 2019 Aug 6; 12(15).
26. Banjanin B., Vladic G., Pál M., Balos S., Dramicanin M., Rackov M., Knezevic I. Consistency analysis of mechanical properties of elements produced by FDM additive manufacturing technology. *Matéria (Rio Janeiro)* 2018;23 doi: 10.1590/s1517-707620180004.0584.
27. Zhang W., Wu A.S., Sun J., Quan Z., Gu B., Sun B., Cotton C., Heider D., Chou T.W. Characterization of residual stress and deformation in additively manufactured ABS polymer and composite specimens. *Compos. Sci. Technol.* 2017;150:102.
28. Singh K. Experimental study to prevent the warping of 3D models in fused deposition modeling. *Int. J. Plast. Technol.* 2018;22:177–184. doi: 10.1007/s12588-018-9206-y.
29. Hong J.H., Yu T., Chen Z., Park S.J., Kim Y.H. Improvement of flexural strength and compressive strength by heat treatment of PLA filament for 3D-printing. *Mod. Phys. Lett. B.* 2019;33:1940025. doi: 10.1142/S0217984919400256

30. Singh S., Singh M., Prakash C., Gupta M.K., Mia M., Singh R. Optimization and reliability analysis to improve surface quality and mechanical characteristics of heat-treated fused filament fabricated parts. *Int. J. Adv. Manuf. Technol.* 2019;102:1521–1536. doi: 10.1007/s00170-018-03276-8
31. Akhoundi B., Nabipour M., Hajami F., Shakoori D. An Experimental Study of Nozzle Temperature and Heat Treatment (Annealing) Effects on Mechanical Properties of High-Temperature Polylactic Acid in Fused Deposition Modeling. *Polym. Eng. Sci.* 2020;60:979–987. doi: 10.1002/pen.25353
32. [Wach R.A., Wolszczak P., Adamus-Wlodarczyk A. Enhancement of Mechanical Properties of FDM-PLA Parts via Thermal Annealing. *Macromol. Mater. Eng.* 2018;303:1800169. doi: 10.1002/mame.201800169.